Ph.D. Dissertation of Natural Sciences

The function of the hippocampal–prefrontal networks in scene–based working memory

해마와 전전두엽 신경 네트워크의 장면 자극 기반 작업기억에서의 기능 연구

February 2023

Graduate School of Natural Sciences
Seoul National University
Brain and Cognitive Sciences Major

Eun-Hye Park

The function of the hippocampal–prefrontal networks in scene–based working memory

Inah Lee

Submitting a Ph.D. Dissertation of
Natural Sciences

December 2022

Graduate School of Natural Sciences
Seoul National University
Brain and Cognitive Sciences Major

Eun-Hye Park

Confirming the Ph.D. Dissertation written by
Eun-Hye Park
December 2022

Chair	이석호	(Seal)
Vice Chair	이인아	(Seal)
Examiner	곽지현	(Seal)
Examiner	이승희	(Seal)
Examiner	박정환	(Seal)

Abstract

Working memory has been described as a function in which stimulus information is maintained even when the stimulus disappears. By maintaining information on stimuli, goal-directed behaviors can be performed, and task-relevant information can be flexibly changed in various environments. It has been known that the function of maintaining and manipulating information is processed in the prefrontal cortex of the brain. In previous studies using monkeys, there was a deficit in performing working memory tasks in the prefrontal lesion group. Also, as a result of electrophysiological measurement of cellular activity in the frontal lobe, it was observed that cellular activity increased and was maintained in the delay period. The frontal lobe also plays an important role in working memory in rats. Previous studies have argued that the hippocampus and prefrontal cortex play important roles, especially based on the fact that place-associated working memory has problems when the connection between the hippocampus and frontal lobe is blocked. However, in these studies, the analysis of what information is maintained and transmitted while working memory is processed has not been properly verified, and network studies between the dorsal hippocampus and prelimbic cortex, which have no direct connection, have been mainly conducted. I focused my research on the CA1 area of the intermediate hippocampus and the network of the infralimbic cortex, which have direct connectivity. It was confirmed that theta waves, which are known as information transfer mediators between the two regions, increased significantly in the delay phase, and it was confirmed that most of the theta phase-locked cells during the delay phase have choice information. Based on this result, it was found that

the relationship between the intermediate hippocampus and infralimbic cortex, unknown in previous studies, plays an important role in the delay phase of working memory, especially in processing choice information.

Keyword : Medial prefrontal cortex, Hippocampus, Working memory, Scene-based task, Virtual Reality
Student Number : 2015-22666

Table of Contents

List of Figures

Background and Hypothesis

Medial Prefrontal Cortex and working memory

Working memory was proposed as a memory of planning future actions to achieve goals. The most important element of working memory is maintaining and manipulating the information when performing the task. Working memory is a cognitive function that allows the brain to temporarily retain information for the task being performed despite the physical disappearance of the information. It is directly related to the ability to perform various goal-directed behaviors. The areas that have been traditionally considered to be responsible for working memory and have been studied a lot are the medial prefrontal cortex (mPFC), medial temporal lobe (MTL), and hippocampus (HPC). It was found in the lesion study that mPFC is important for working memory. (Pribram et al., 1952; Mishkin and Pribram, 1956) In this lesion study, the performance was decreased in the mPFC lesioned monkeys. Physiological evidence of the prefrontal cortex was presented by maintaining the firing rate during the delay period in monkeys performing a non-match to sample task with a delay (Fuster and Alexander, 1971; Kubota and Niki, 1971; Funahashi et al., 1989). In this study, the cells showing sustained activity in the delay period were defined as cells representing the working memory. Patients or animals with mPFC damage have difficulties in performing planned behaviors and flexibly modifying behaviors using changed information (Milner, 1963; Kolb, 1990; Stuss and Alexander, 2000). People or animals with HPC damage in the MTL suffer, especially when they need to utilize working memory for different spaces. There are some objections about the persistent

activity being the physiological evidence of working memory (Miller et al., 2018). They argued that persistent activity is vulnerable to noise and needs a lot of energy to maintain the activity. They hypothesize that mPFC cells not just maintain but process the task-relevant information along the working memory task. For these reasons, they verify the information processing in the working memory task (Wallis et al., 2001; Freedman et al., 2002; Nieder et al., 2002). Even in rats lesioned with HPC, it was difficult to perform the spatial working memory task (Eichenbaum, 2000; Lee and Kesner, 2003; Lee and Solivan, 2008). If the circuit between HPC and mPFC is disconnected, the performance of working memory tasks decreases (Spellman et al., 2015). Experimental evidence has been reported that neural network activity between mPFC and HPC is important for hippocampal-dependent working memory task performance (Spellman et al., 2015; Shin et al., 2019). For the past decade, only theoretical explanations have been attempted on the mechanism of maintaining working memory in neural networks (Baddeley and Hitch, 1974), and there have been no attempts to establish a theory based on the biological characteristics of neurons or neural networks of mPFC or to verify them experimentally. Therefore, it is necessary to investigate which physiological mechanism is implemented in the mPFC neural network to maintain the corresponding memory during the working period and where the mPFC receives the task-relevant information.

Different functions of the mPFC subregions

Prelimbic(PL) and Infralimbic(IL) are known subregions of the mPFC. The two regions are known to play different roles, especially in fear memory. The PL plays an important role in fear memory acquisition, while the IL plays an important role in fear memory extinction (Sierra-Mercado et al., 2011; Marek et al., 2018). In addition to Fear memory, it is known that the mPFC is involved in the flexible reversal of its own response. In particular, the IL is important for reversal learning, and the PL is not involved in reversal learning. On the other hand, in Mukherjee and Caroni(2018), the PL plays an important role in intradimensional shift when it is necessary to re-associate one's choice within the learned rule, and the IL plays an important role when reward and non-reward cues are switched. The two regions are anatomically different. The main difference is the connection from the hippocampus. Both regions receive direct projection from the HPC, but the PL mainly receives projection to deep layers (layers 5 and 6), and the IL receives projection to all layers (Figure 1) (Hoover and Vertes,(2007); Liu and Carter, 2018). It is thought that the HPC to the PL and the HPC to the IL might have different functions because they receive information differently from the HPC, an area that processes information about the environment and episodic memory. There is a rare projection from the dHPC to the mPFC; nevertheless, most of the studies about the function of the network from HPC to PFC targeted the dHPC and PL (Tang et al., 2017; Shin et al., 2019). Zielinski et al., (2019) show that the PL and dHPC show planning of the future route.

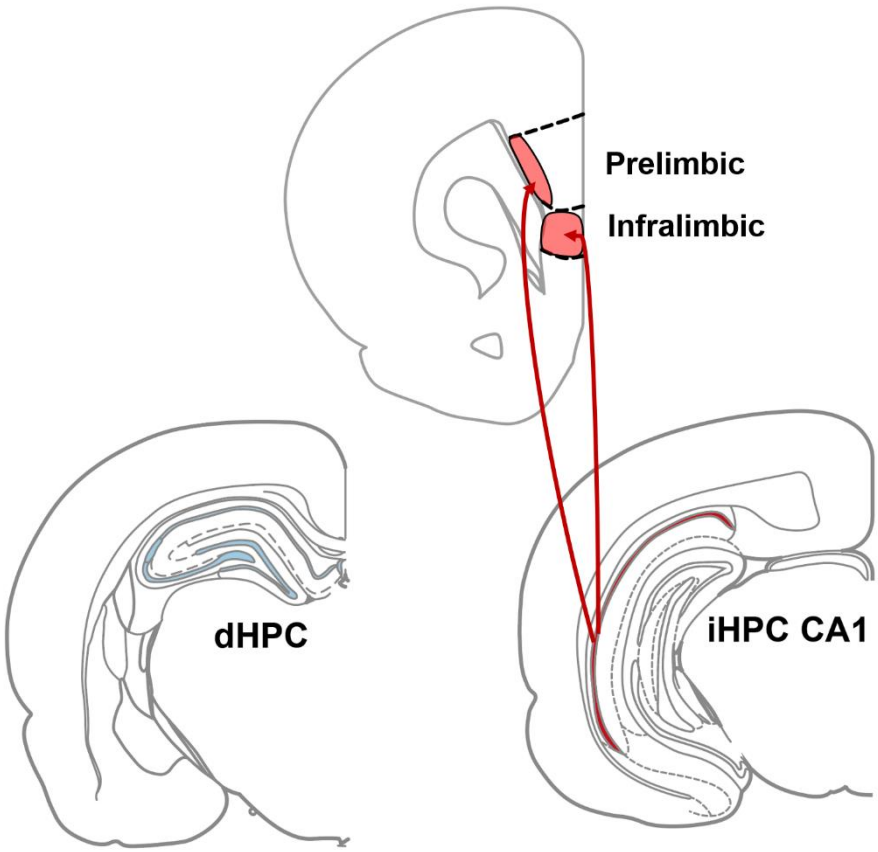

Figure 1. Afferent projection from the iHPC to the mPFC

There is a direct projection from the iHPC to the IL and PL. Especially both deep and superficial layers of the IL receive the iHPC projection. However, in the PL, only the deep layer is projected from the iHPC. Also, there is a rare projection from the HPC to the mPFC. The rat brain atlas is adapted from Paxinos and Watson(2009)

Hippocampus and Episodic memory

As a result of observing the behavior of HM patients whose HPC was surgically removed, HM showed anterograde amnesia and had no problem in motor skill learning (Scoville and Milner, 1957). Through these results, it was known that HPC plays an important role in episodic memory. In the lesioned rodent of HPC, behavioral problems arose in the formation of spatial and sequential memory (Eichenbaum, 2000; Macdonald et al., 2011). It was also found that electrophysiologically recorded HPC cells contain contextual scene information (Lee et al., 2018; Lee and Lee, 2020; Shin et al., 2022). Through this, HPC and its surrounding area, the medial temporal lobe, play important roles in episodic memory (Ahn and Lee, 2017; Yoo and Lee, 2017; Park et al., 2017). The physiology studies show that the HPC encodes the different episodic memory in the same location (Wood et al., 2000). Also, the HPC encodes the phase-specific information (Carr et al., 2011) in the delayed non-match to sample task, during the sample and delay phases (Otto and Eichenbaum, 1992). These results indicate that the HPC processes not just spatial information but also episodic memory (Eichenbaum et al., 1999).

Spatial and value representation in the hippocampus

Traditionally the HPC is important for place information processing(O'keefe and Dostrovsky, 1971). There are place cells active in the focal position of the place in the dorsal HPC (dHPC) (Muller and Kubie, 1987). Whereas in the intermediate HPC(iHPC),

the place field is broader than the dHPC (Jung et al., 1994), and the emotional value information exists. Jin and Lee (2021) performed the place-value association task and recorded the cell activities in the iHPC and dHPC simultaneously. In this paper, the iHPC shifted its field more rapidly than the dHPC. This result indicates that the iHPC is important for the spatial-value association. Also, Bast et al. (2009) argue that the iHPC plays an important role in rapidly learning the water maze task. These results suggest that the iHPC is important for the rapidly changing place-value association for goal-directed behavior.

Planning the route for arriving at the goal location and maintaining the information until achieving a goal are important factors in working memory tasks. Therefore, the iHPC, which is the region of the task-relevant value information processing, is critical for the working memory. The Burton et al (2009) show that the lesion of the iHPC disrupted the anticipatory reward activity in the mPFC. This result indicates that the iHPC is an important source for goal-directed action planning and working memory information processing in the mPFC (Hok et al,, 2005).

Hippocampus and working memory

Previous studies show that the HPC also plays an important role in working memory (Watanabe and Niki, 1985). In Lee and Kesner (2002, 2003), the rats performed the delayed non-matching to place task. In this study, the dHPC lesion group shows performance deficits in the spatial working memory task. Also, in Spellman et al (2015),

the mice performed the delayed spatial alternation task in the T-maze and inactivated the ventral HPC(vHPC) to the mPFC circuit using optogenetics. In this paper, the vHPC to mPFC circuit inactivation shows performance deficits in the sample phase. Jones and Wilson (2005) show that the dHPC and mPFC are highly coherent in theta frequency in the delay phase of the working memory task. These results indicate that the HPC affects the working memory task, especially the encoding period.

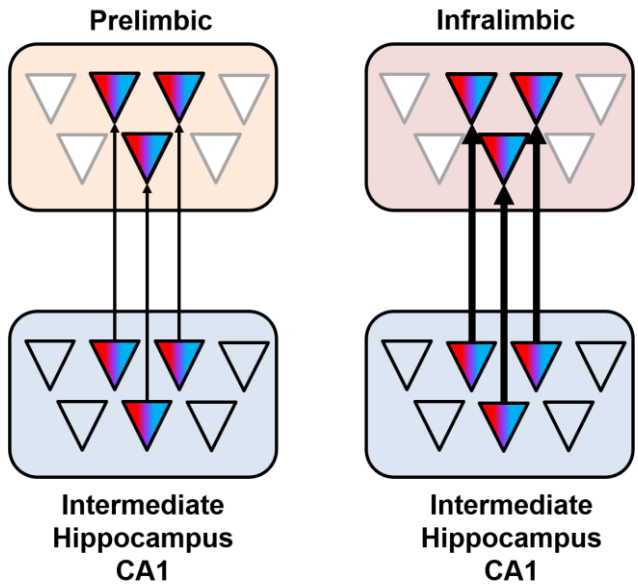

Figure 2. Hypothesis

Hypothesis

In the working memory task, the infralimbic cortex is more affected by the iHPC inactivation than the Prelimbic cortex. Also, the iHPC to the IL circuit is important for the task-relevant information processing.

Chapter 1

1.1 Introduction

HPC is known to play an important role in processing spatial information (O'keefe and Nadel, 1978; Olton and Werz, 1978; Morris et al., 1982), especially the iHPC is important in associating space and value information (Jin and Lee, 2021). Therefore, it is expected that the network function of the iHPC to mPFC plays an important role in processing environment-associated choice information when performing working memory (Burton et al., 2009). Previous studies used delayed non-match-to-sample tests with simple sensory cues to test networks in these two areas (Spellman et al., 2015). However, in order to test the functions of the HPC and mPFC, a scene-based working memory test should be performed. To test this hypothesis, rats were trained the scene-based working memory task. In this task, rats should see the scene in the sample phase, and they maintained the information until the response phase was started. They should be able to process the appropriate information according to the time sequence. Also, They should be able to maintain the scene-associated choice information during one trial and flexibly change their information in the next trial. Therefore, four different environments were created in the VR space, and the rat was trained the response according to each environment. In rats performing the scene-based working memory task, CA1 of iHPC, which is the efferent projection area to mPFC, was inactivated, and behavioral changes were examined.

1.2 Materials and Methods

1.2.1 Subjects

Five Male Long-Evans rats were housed individually in plexiglass cages in a temperature- and humidity-controlled animal colony. Rats were maintained on a 12hr light/dark cycle, and experiments were carried out in the light phase of the cycle. Rats were food-restricted to maintain 80% of their free-feeding weight but allowed water freely. All protocols used are in compliance with the Institutional Animal Care and Use Committee of Seoul National University.

1.2.2 Virtual Reality System

VR environments consisted of a linear track with various visual object cues placed using Unreal Engine 4.14 (Epic games, Inc) (Figure 3A). There are four different environments in VR space (Forest, City, Playground, and Room) (Figure 3B). Rats were body-fixed on the aluminum profile structure above the styrofoam wheels. Rats can move forward in virtual space by rolling the wheel. There are three 24-inch LCD monitors around the rat to cover approximately 270 degrees of the rat's view, and virtual space is presented on the monitor. There are licking ports on the left and right sides of the rat. Each licking port has a proximity sensor that can detect the rat's licking behavior. Honey water comes out of the licking port to reward rats. The amount of honey water was regulated via a solenoid valve controlled by the Arduino. The sensors send the rat's behavioral data to the computer using Arduino. Also, Arduino generated TTL signals

for interworking between Neuralynx and UE programs. The VR system was placed in the (121 cm x 136 cm x 246 cm) of a soundproof booth, and white noise was played during the behavioral experiment to mask the sound noise from outside.

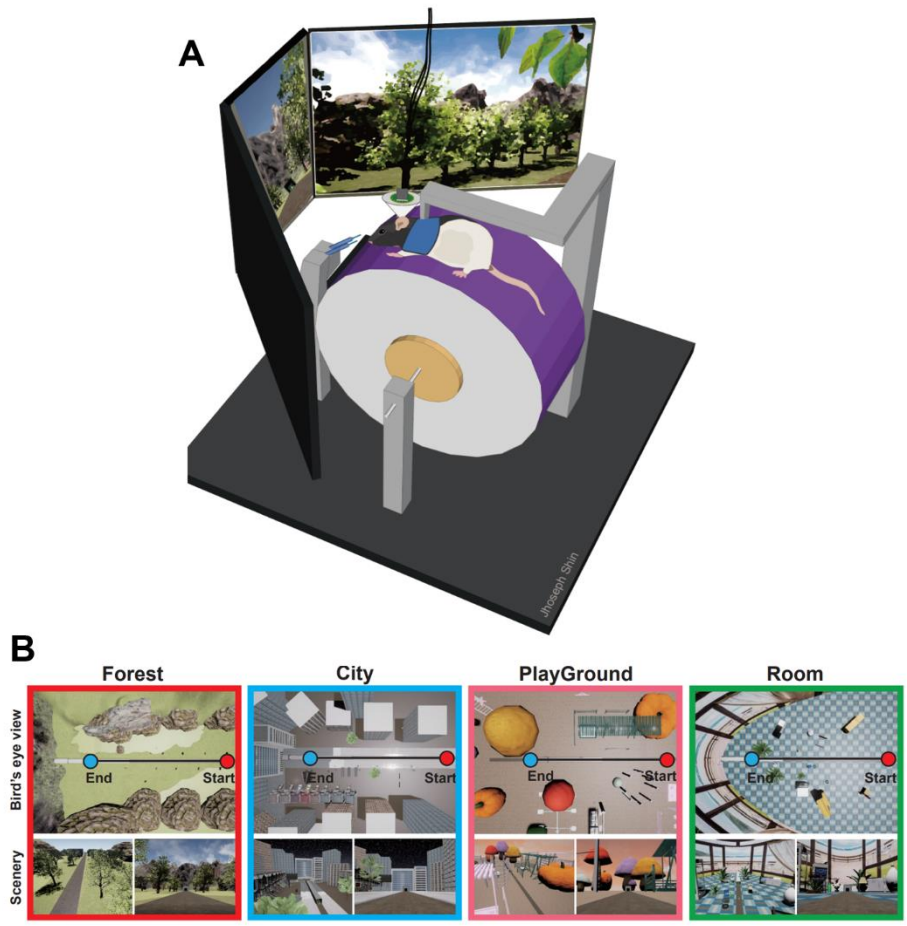

Figure 3. Virtual Reality system.

(A)Rats were body-fixed on the aluminium structure above the wheel. There are three LCD monitors around the rat and the VR space is presented on the monitors. The two licking ports are positioned on the left and right sides of the rat. (B)There are 4 VR environments, Forest, City, Playground, and Room. Rats started from the position of the red circle and end the position of the blue circle. The environments consist of many objects.

1.2.3 Handling and familiarization

Naive rats were handled on a towel for 30 min per day to adapt to the experimenter and to the licking of honey water in a syringe. When the rat got more than 7ml of honey water per day, it met the criteria. After the towel handling phase, rats were handled in the VR booth putting the harness on to acclimate to the VR system. Once the rat consumed over 7ml of honey water in the VR booth, a simple association task phase began.

1.2.4 Simple association task

The rats were trained in a simple association task to make the rat run on the linear track and lick the left and right ports in the VR environment. In this period, the VR environment consisted of a linear track with no object. When the rat arrived at the tunnel, which is positioned at the end of the route, the rat was transported to the start position for the next trial. The 30μL of honey water rewards were given pseudo-randomly placed on the route in each trial on the left and right sides of licking ports. The liking ports were placed out of reach of the rat and became close to possible to lick using the linear motor when the rat arrived at the reward location. The rats were trained until they ran over 100 meters in 30 minutes and consumed rewards on the licking ports.

1.2.5 Scene-based no-delay task

After the simple association task, rats were trained in a scene-based no-delay (SND) task. In this task, two different environments (set

of Forest and City or set of Playground and Room) were presented, and each environment was associated with the left or right side of the licking port. Rats ran through the environment and were transported to the response zone (gray tunnel) when they reached the end of the environment. Rats should lick the correct side of the reward port immediately after transport to the response zone based on the environmental scene to get 30μL honey water rewards. After the reward period, the rats were transported to the black tunnel, which is Inter-Trial-Interval (ITI). The subsequent trial is initiated after 2 seconds from the ITI start. Rats conducted 120 trials a day, 60 trials per environment. The sequence of environments is pseudo-randomly presented. The performance criteria are greater than 70% correct trials per environment or above 70% correct trials on average for all environments, with a response bias of less than 0.15 for two consecutive days.

1.2.6 Scene-based working memory task

When the rats reached the criteria in the SND task, they were trained in a scene-based delay (SD) task. The difference between the SND and SD task is the delay period(3s) is presented before the response phase in the SD task (Figure 4). The rat should lick the correct side of the licking port based on the environmental scene after the 3s delay to get 30μL of honey water rewards (Figure 4A). When the rats got to the criteria for two consecutive days, they were trained the second set of environments in the same training sequence as the first set. After the performance of the second set satisfied the criteria

for two days in a row, the rats were trained in four environments (all of the first and second sets of environments) 120 trials per day, 30 trials per environment in the SD task (Figure 4B).

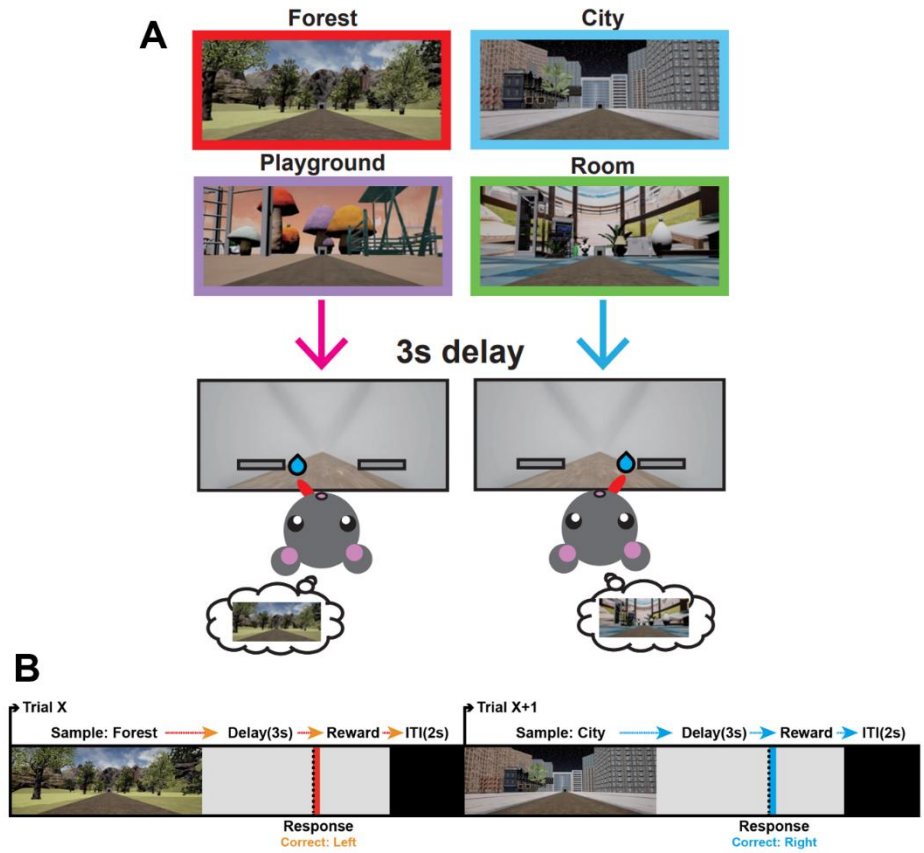

Figure 4. Behavior paradigm and sequence of trial.

(A) After the 3s delay, rats should lick correct side of the lick port to get a reward according to the scene. (B) The task trial consists of 5 phases. First, in the sample phase, rats were sampling the scene. Second, there is 3s delay phase after the sample phase. Third, the response phase is started after the delay phase. Fourth, some honey water rewards were given to the rat when the rat chose the correct side of the licking port. Fifth, there is the ITI phase during the 2s.

1.2.7 Surgery

When the rat satisfied the criteria in the SD task training, I implanted bilateral cannulae in the iHPC and, simultaneously, a hyperdrive carrying 24 tetrodes in the mPFC to record the single-unit neuronal spiking activity (Figure 5). Each tetrode was adjusted to 100-300kΩ of impedance. The Nembutal deeply anesthetized rats with an intraperitoneal injection (65mg/kg). Anesthesia was maintained using isoflurane which was 0.5-2% mixed with 100% oxygen during the surgery. The Head was fixed to the stereotactic arm (Kopf Instruments, USA), and the skull was exposed after the incising of the scalp. Two small burr holes were drilled, and cannulae were implanted in the iHPC bilaterally. The following coordinates were used: AP -5.52mm, ML±6.1mm, DV-4.6mm from the dura. A burr drilled the hole for the hyperdrive bundle. Hyperdrive was implanted in the right hemisphere of the brain, and the bundle tilted laterally at 10 degrees. The center of the tetrode bundle was placed AP+3.24mm, ML-1.8mm. The hyperdrive and cannulae were chronically fixed to the skull with eight fixing screws and bone cement. All tetrodes were lowered by 1.0 mm immediately after the surgery. Rats were given 6 days to recover from surgery.

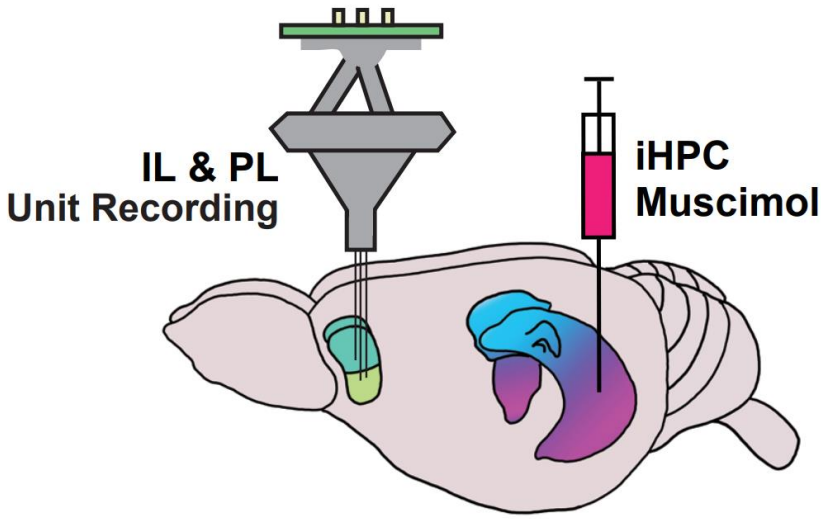

Figure 5. Implantation of hyperdrive in the mPFC and cannula in the iHPC.

The hyperdrive was implanted in the right hemisphere and simultaneously the cannulae were implanted into the iHPC bilaterally.

1.2.8 Postsurgical re-training procedure

After a week of the recovery period, rats were re-trained SND task with 4 environments, 120 trials per day, and 30 trials per environment. They were trained SD task in 4 environments when they reached the pre-surgical criteria in the SND task. When the rats got the pre-surgical criteria in the SD task, the neural activities recording and drug injection session was begun. Over this re-training period, tetrodes were slowly lowered down the target regions. And a reference electrode was placed in the fiber zone. In order to adjust the tetrodes, each rat was placed in the small booth outside the behavior VR room. Digitalized and 1000-10,000 times amplified neural activities were sent through the headstage (Neuralynx). The tether interfaces the information from the headstage of the hyperdrive to the digital acquisition system (Cheetah system).

1.2.9 Drug injection procedure

On the next day of the rats satisfied the criteria in the re-training, the rat was injected with the Phosphate Buffered Saline (PBS) into the iHPC bilaterally (0.5 μL per site) 20 minutes before behavioral testing. On the next day, the same rat was injected with the GABA-A receptor agonist Muscimol (MUS) into the iHPC (0.5 μL per site). This PBS and Mus injection sequence was repeated 1 more sets.

1.2.10 Histology

When all recording sessions were completed, an electrolytic lesion was conducted via each tetrode (10 μA current for 10s) to mark the tetrode tip position. 24 hours after the electrolytic lesion, fluorophore-conjugated muscimol (f-MUS; Sigma, USA) was injected bilaterally in iHPC (0.5 μL per site) to verify the spread range of the MUS. 20 minutes after the f-MUS injection, the rat inhaled an overdose of CO_2 and was perfused transcardially, first with 60ml of PBS with syringes and then with 300ml of 4% v/v formaldehyde solution at a constant speed. The fixated brain was extracted from the skull and post-fixed in 4% v/v formaldehyde-30% sucrose solution at 4° C for 2-3 days. After post-fixation procedures, the brain was gelatin-coated and soaked in 4% v/v formaldehyde-30% sucrose solution for 1 day. The brain was sectioned at 40 μm using a freezing microtome (HM 430; Thermo-Fisher Scientific). Brain sections were mounted on the subbed slide glasses and dried. 1 day after the mounting, the brain sections were taken fluorescent micrographs of the f-Mus with a digital camera attached to a fluorescent microscope (Eclipse 80i, Nikon). After the fluorescent micrography, the brain tissues were stained with a thionin solution. Photomicrographs of thionin-stained brain tissues were taken using a digital camera. The tetrode tips were reconstructed three-dimensionally. The reconstructions of locations of tetrodes were determined using the 3D images and physiological depth profiles recorded during cell activity acquisition.

1.3. Results

1.3.1 Histological Results

The position of the tetrode tips of each rat was verified. The location of the tetrode tips of each rat was marked with different colors on the rat brain atlas (Figure 6). The positions of tetrode tips were distributed from +4.2 to +2.5 from the bregma. PL and IL are subregions of mPFC (Figure 6A). The criterion for the boundary of PL and IL was based on the thickness of layer 2. In the previous study, layer 2 in PL is more compressed and thinner than the IL. In the PL, 49 cells were recorded in a PBS session, and in a MUS session, 41 cells were recorded. In the IL PBS session, 39 cells were recorded, and in the MUS session, 32 cells were recorded. Also, the locations of the bilateral cannula tips were verified (Figure 6B). All cannula tips were located in the CA1 of iHPC. Since most HPC to mPFC projections is started from the iHPC CA1 area, the CA1 should be targeted to disconnect the two areas.

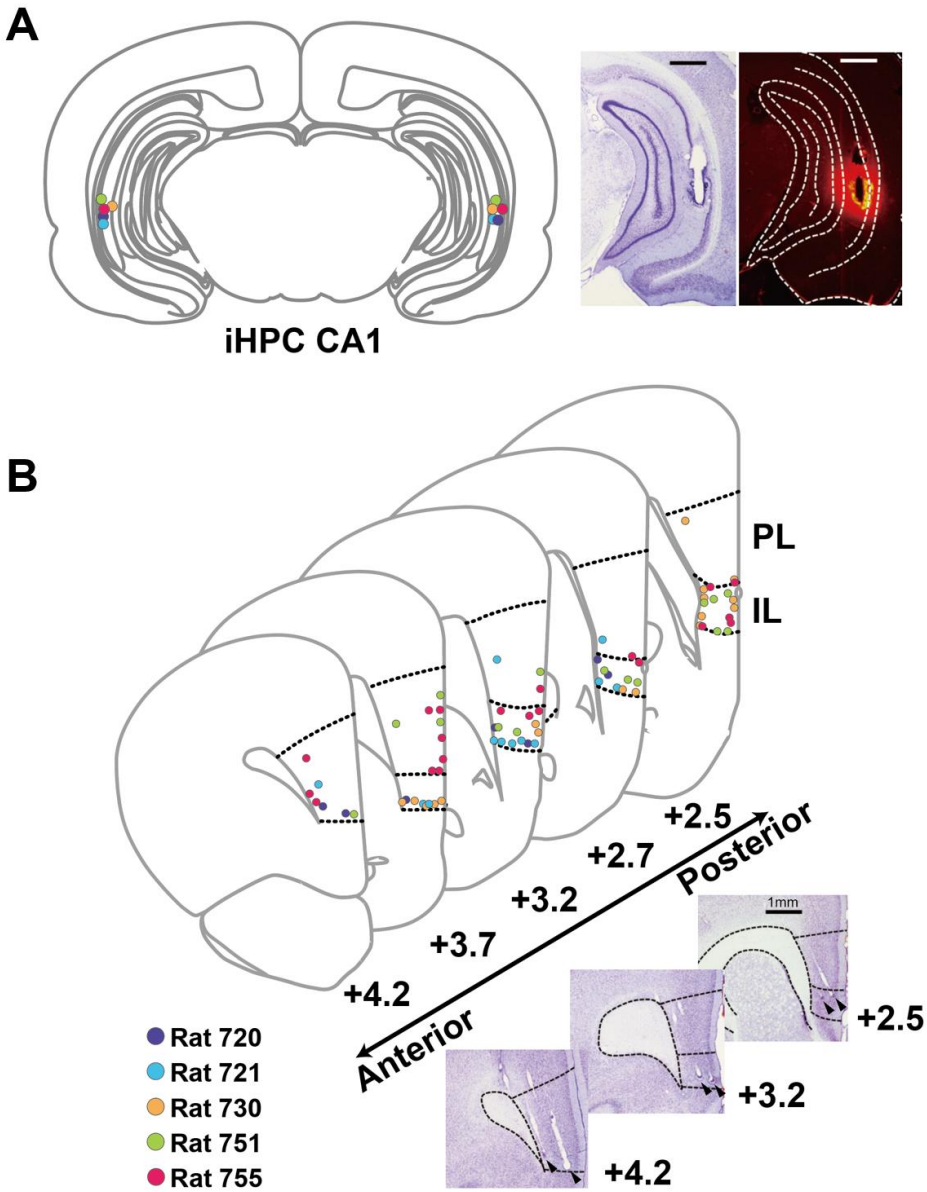

Figure 6. The positions of the cannulae tip and tetrode tip were verified.

(A) The cannula tip positions into the iHPC, and the coverage of the f-MUS is verified. Each rat's cannula position is color coded. (B) The tetrode tip positions into the mPFC of each rat are verified.

The rat brain atlas is adapted from Paxinos and Watson(2009)

1.3.2 Behavioral results

Injection of MUS into the iHPC CA1 resulted in significant performance deficits compared with injection of the same volume of PBS (Figure 7). Paired t-test showed a significant decrease in percent correctness in the MUS groups (p-val<0.001; paired t-test) (Figure 7A). Also, the choice bias showed a significant difference in the MUS group (Figure 7B). Paired t-test showed a significant increase in bias in the MUS groups (p-val<0.01; paired t-test). These results suggest that iHPC CA1 may play an important role in a scene-based working memory task.

However, the running speed in the sample phase and the licking latency in the response phase was no difference between the PBS and MUS groups. Paired t-test in running speed is not significantly different in PBS and MUS (Figure 8), and also, the licking latency is not significantly different in PBS and MUS (Figure 7C). These results show that the MUS can not affect the general motor movement in the scene-based working memory task.

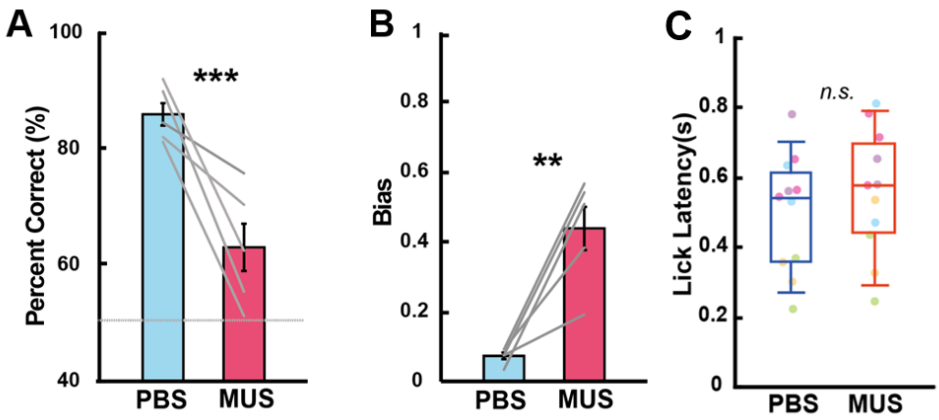

Figure 7. Behavioral results in a scene-based working memory task.

(A) The percent correctness is a significant difference between the PBS and MUS sessions in the scene-based working memory task. Each rat's performance is plotted by the gray line. (B) The choice bias is significantly different between the PBS and MUS sessions. (C) Licking latency in the response phase is not different in the two sessions.

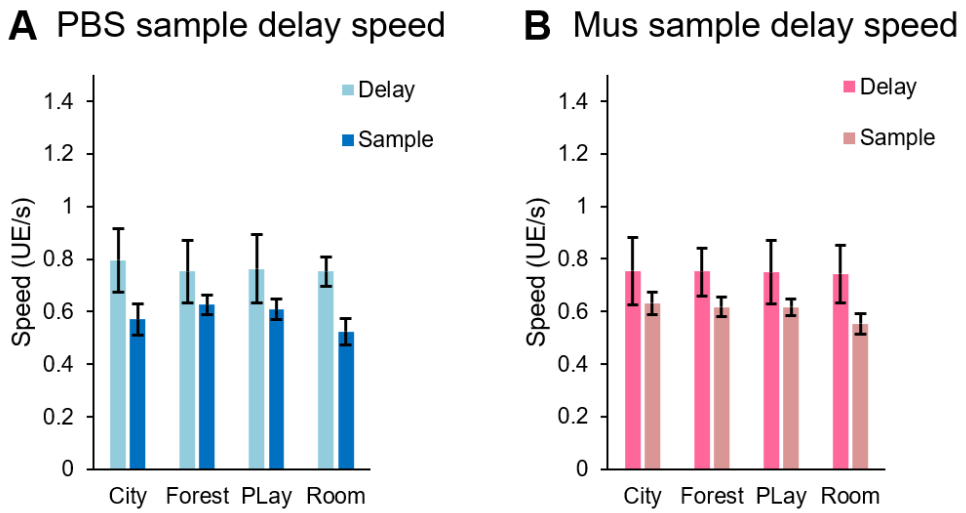

Figure 8. Running speed in the sample and delay phases are not different.

(A) The running speed in the delay and sample phase in the PBS session. In each scene phase, the speed in the sample and delay phases are similar. (B) Same as the (A) but in the MUS session.

1.4 Discussion

When CA1 of iHPC was inactivated, the scene-based working memory task showed significant behavioral deficits. From this result, the CA1 of iHPC is essential for scene-based working memory. Anatomically, the iHPC receives direct projection from CA3 of the dHPC and direction projection from the amygdala (Pitkänen et al., 2000) and VTA (Lisman and Grace, 2005), the area processing the emotional information. Based on the anatomical circuit, the iHPC might receive spatial information from the dHPC and receive the value information from the amygdala and VTA. It is possible that the spatial associated value information is formed in the iHPC by synthesizing the information from the dHPC and amygdala. In the Jin and lee (2021), they argued that the role of HPC according to the longitudinal axis is different. In particular, the iHPC is expected to have an association between spatial information and value information. Also, they assumed that associated spatial information and value information in the iHPC would be delivered to mPFC to select the action. Since the CA1 of the iHPC processed the scene-related value information, it can be interpreted that significant results were found in the scene-based working memory when the iHPC was inactivated. The projection from the dHPC to the mPFC rarely exists. However, the amount of projection from the iHPC to the mPFC is larger than the dHPC. Therefore, the spatial-value information from the iHPC is more important than the spatial information from the dHPC in the mPFC. The information from the iHPC is important in the mPFC

because appropriate action to the environment plays an important role in the mPFC. In Chapter 2, mPFC cells were recorded during a scene-based working memory task to test what information the iHPC sends to the mPFC and what disappears from the mPFC.

Chapter 2

2.1 Introduction

The mPFC is known to play an important role in flexible behavior (Milner, 1963), executive monitoring (Norman and Shallice, 1980), and working memory (Fuster and Alexander, 1971; Lee and Kesner, 2003). Flexible behavior means changing the response according to the space or cue to adapt to the environmental change effectively. Executive monitoring means keeping watch of activities of the brain area to synchronize the areas within a learned rule. These two roles of mPFC are critical for working memory. In the working memory, temporally organizing the event phase by the learned rule (i.e., Sample-Delay-Response) and flexibly alternating the response to the changing environment (i.e., Forest-Left, City-Right) are two critical factors. In the previous study (Mukherjee and Caroni, 2018), the PL is important for the new learning within the learned rule, and the IL plays a crucial role in flexible alternation. Therefore, I hypothesize that the PL is important for the temporal organization in the working memory task, and the IL is important for the appropriate action according to the environment. Anatomically the PL and IL have a reciprocal connection (Hoover and Vertes, 2007). These two regions communicate to conduct the goal-directed working memory task. The iHPC is known as a spatial value information association area (Jin and Lee, 2021), and projects to the IL and PL directly (Liu and Carter, 2018). In the previous paper, the iHPC to mPFC circuit is important for the spatial-working memory (Spellman et al., 2015). But in the previous paper, what information is sent to the mPFC from

the iHPC was not reported. Also, the mPFC is known for maintaining task-relevant information in the delay period (Funahashi et al., 1989), but what information was maintained is not verified. I hypothesize that the information from the iHPC to the mPFC is spatial-associated response information to process the appropriate action according to the environment.

2.2 Materials and Methods

2.2.1 Electrophysiology recording

Concurrently with the drug injection procedure, the electrophysiological recording was conducted in the SD task. 20 minutes after the drug injection, the rats were body-fixed on the VR system and performed the SD task in 120 trials of 4 scenes. During the behavioral task, neural signals were acquired to the Neuralynx system. Neural signals were digitized at 32kHz (filtered at 600-6,000 Hz).

2.2.2 Unit isolation

Single units were simultaneously recorded from the PL (PBS session: n=49; MUS session: n=41) and IL (PBS session: n=39; MUS session: n=32) cortex. These cells are manually isolated with custom-written software (WinClust) using the multiple waveform parameters as previously described (Lee and Kim, 2010; Delcasso et al., 2014). Neurons were excluded that did not satisfy the criteria: (i) the proportion of spikes recorded during the 1ms refractory period was less than 1% of total spikes (ii) the average peak-to-valley amplitude of waveforms was greater than 75μV, (iii) the average firing rate within the trial was greater than 1Hz. Cells with an average firing rate exceeding 10Hz and width of the average waveform less than 325μs were classified as fast-spiking neurons, and these neurons were excluded.

2.2.3 Basic firing properties

Single unit cells from the PL and IL were grouped into bursting cell, regular-spiking cell, and unclassified cell. The bursting cells are classified when they meet the criterion from the counts in their autocorrelograms(max(3-5ms)>max(0-50ms)/2). Among the non-bursting neurons, regular spiking cells are dissociated based on the interspike interval histogram < 35ms. These cell classification criteria are based on the previous study (Barthó et al., 2004).

2.2.4 Rate map construction

I divided the trial into three sequential task-relevant phases the Sample phase, Delay phase, and Response phase. The sample phase consisted of the start of the 4 scenes to the end of the scenes. Right after the end of the sample phase, the delay phase is begun. The response phase is started 3 seconds after the start of the delay phase. When the rat lick the left or right licking port, the response phase is over. For the construction of the rate map, the length of the sample phase track was divided into spatial bins. The firing rate of each bin was calculated by dividing the number of spikes by the duration of occupancy for the bin. The adaptive binning method (Skaggs and McNaughton, 1993) was used to smooth the raw rate map. In the delay phase, the 3 seconds time was divided into time bins. The firing rate of each bin was calculated by dividing the number of spikes. The response phase was not divided, and calculated the firing rate from phase start to end. I smooth the raw rate map in the delay and response phase with the moving time window smoothing method.

2.2.5 Rate difference index (RDI)

To obtain the amount of rate modulation between rate maps of scene trials, RDI was calculated (Figure 9) by computing an absolute value of Cohen's d:

$$\text{Rate Difference Index} = \left| \frac{mean(\text{FR1}) - mean(\text{FR2})}{std(\text{FR1},\text{FR2})} \right|$$

FR1 and FR2 represent the firing rates of the trials of two different conditions (e.g., Forest vs. Playground scene trials; City vs Room scene trials), respectively. The Choice information (RDIchc) is calculated by the difference in firing rates between the left and right response trials. Also, the difference between firing rates in the Scene information (RDIscn) was computed with different scenes sharing the same choice response trials. And then, the maximum value of the right and left scene information was taken.

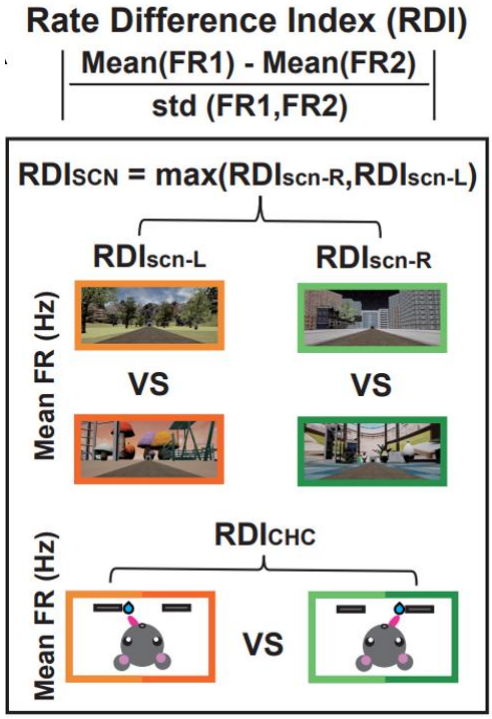

Figure 9. RDI was calculated by computing an absolute value of Cohen's d.

2.2.6 Angle value calculation

The angle value is calculated as the tanθ of the plot position. The RDIchc value is divided by the RDIscn value of the plot position.

$$\tan\theta = \frac{\text{RDIchc value}}{\text{RDIscn value}}$$

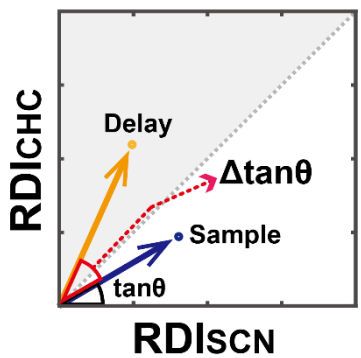

Figure 10. Angle value calculation.

The $\tan\theta$ is the value of the angle that is RDIscn and RDIchc position of each cell. The $\Delta\tan\theta$ is the amount of angle change between the two phases.

2.3 Results

2.3.1 Basic firing properties of the PL and IL.

The number of cells that satisfied the criterion in the PL is 90 and in the IL is 71 (PL PBS: n=49; PL MUS: n=41; IL PBS: n=39; IL MUS: n=32). The bursting cells and the regular spiking cells are dissociated in the PL and IL based on the previous study (Bartho et al., 2004) (Figure 12). In the PL, there are 34.7% of bursting cells, 61.2% of regular spiking cells, and 4.1% of non-classified cells. These proportions are not different between the PBS and MUS sessions (Figure 13). In the IL, there are 33.3% of bursting cells and 66.7% of regular spiking cells. To verified the basic cell firing properties in the mPFC is not affected by the iHPC MUS sessions, I calculated the peak firing rate(Hz), mean firing rate(Hz), and spike width (μs) in the iHPC PBS and MUS sessions. These basic firing properties between the PBS and MUS sessions are not significantly different (Figure 15 A-F). There is a slightly decreased in the Mean firing rate in the IL, but this result is not significant statistically(Z=0.8032, p-val=0.4219; Wilcoxon Ranksum test). These results indicate that the basic cell activities do not change even when the iHPC is inactivated.

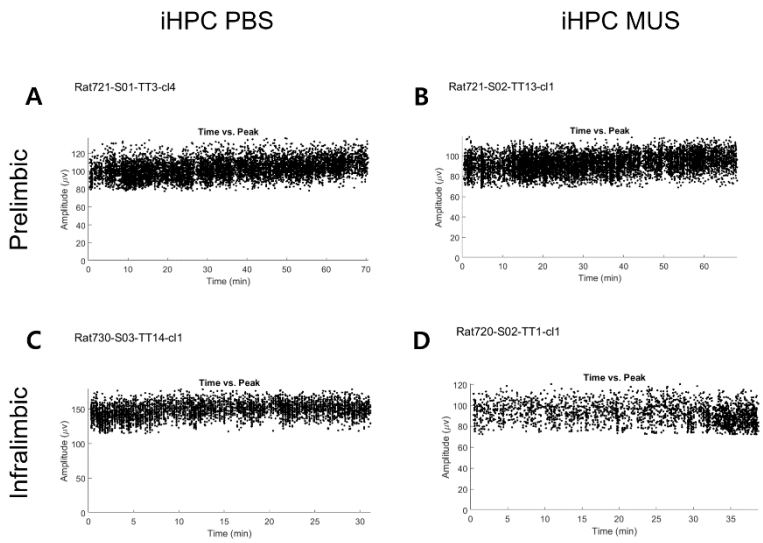

Figure 11. The amplitude of the PL and IL cells during the behavioral task.

(A) Examples of the amplitude of the PL cells in the iHPC PBS session. (B) The amplitude of the PL cells in the iHPC MUS session. (C) The amplitude of the IL cells in the iHPC PBS session. (D) The amplitude of the IL cells in the iHPC MUS session.

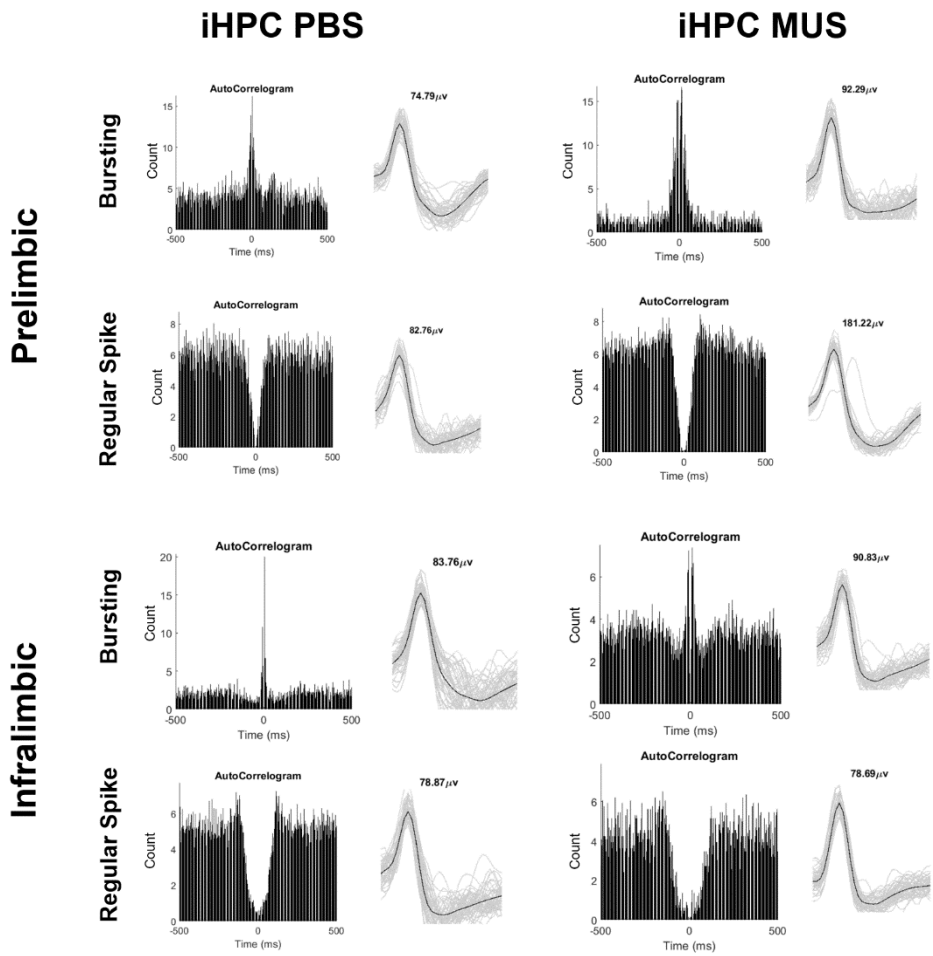

Figure 12. Representative autocorrelograms and waveforms of the PL and IL cells.

There are two types of cells in the PL and IL cells during the working memory task. The bursting cells and the regular spiking cells are dissociated in the PL and IL based on the previous study (Barthó et al., 2004).

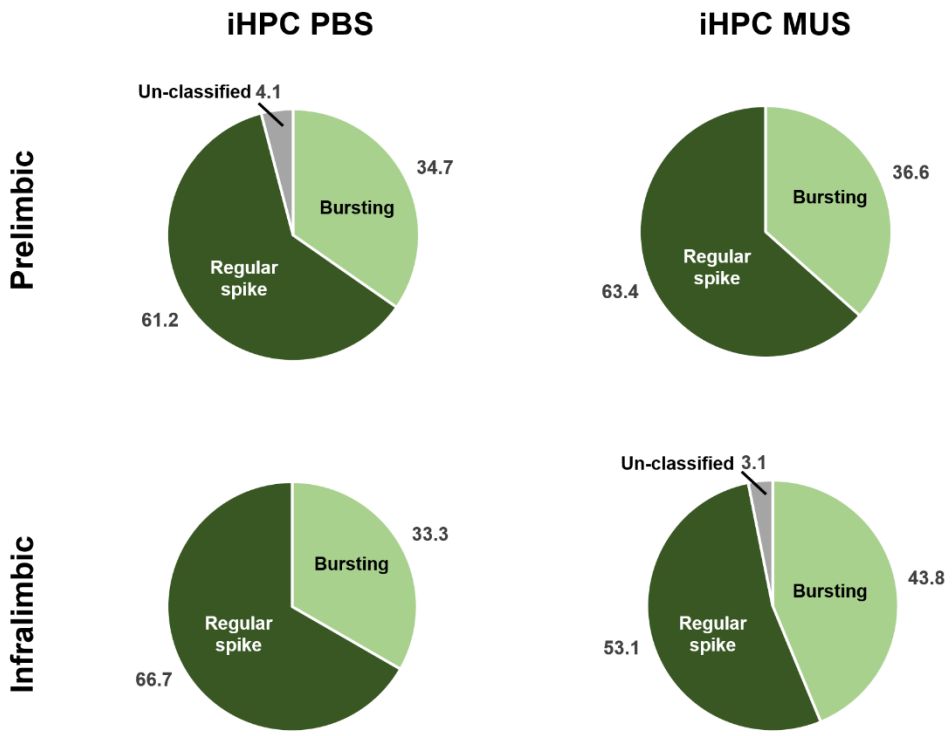

Figure 13. The proportion of the cell types in the PL and IL.

Pie charts show the proportion of the bursting, the regular spiking cells, and the un-classified cells in the PL and IL. There is no significant difference between the iHPC PBS and iHPC MUS sessions.

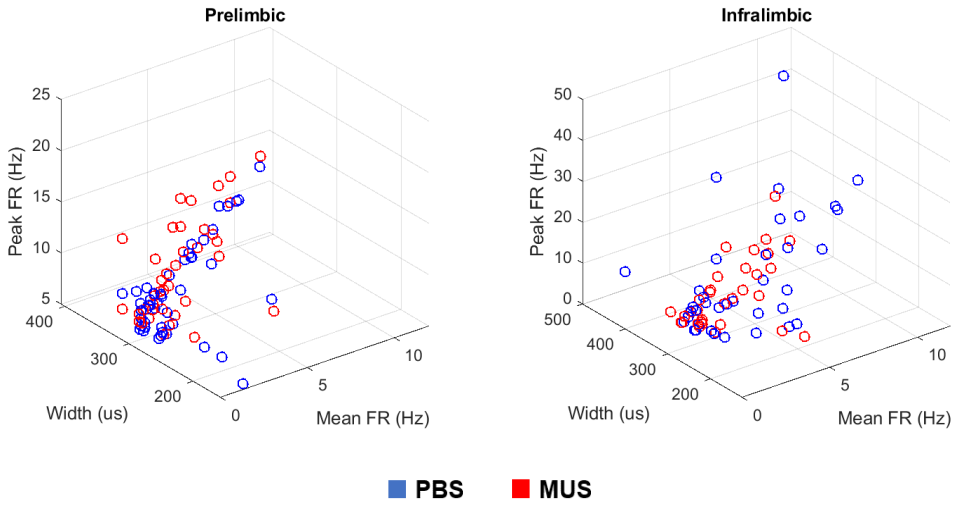

Figure 14. Plots of the basic firing property of each cell.

This 3D graph shows the mean firing rate (Hz), the peak firing rate (Hz), and the Width (ms) of the PL and IL cells. Each dot means one cell. (PL PBS: n=49; PL MUS: n=41; IL PBS: n=39; IL MUS: n=32).

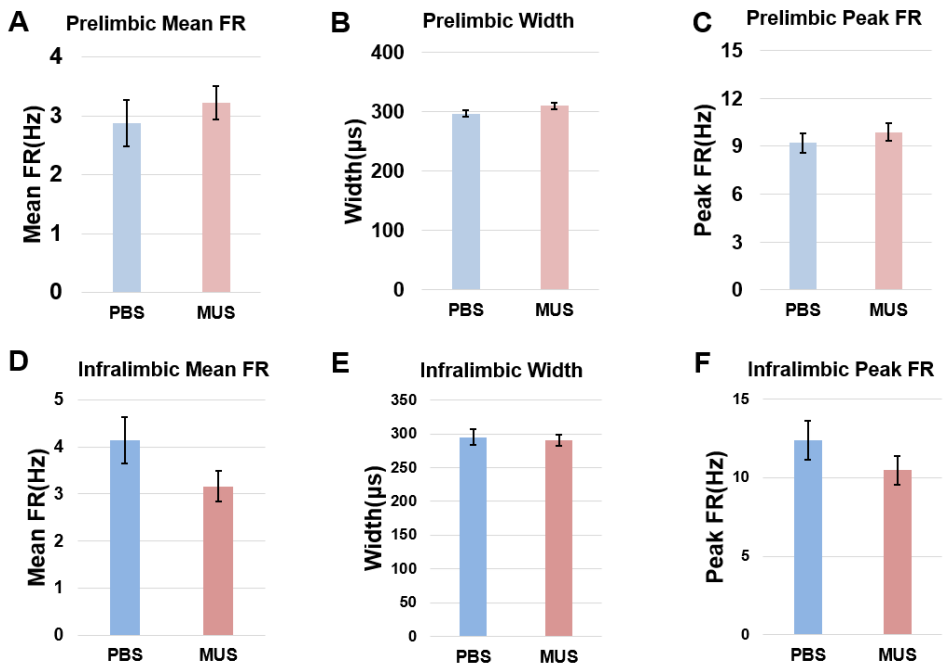

Figure 15. Basic firing properties are not different between the PBS and MUS sessions.

(A) The Mean firing rate (Hz) is not significantly different between the PBS and MUS sessions in the PL. (B) Spike width(μs) (C) Peak firing rate (Hz). (D) (Z=0.8032, p-val=0.4219; Wilcoxon Ranksum test), (E), (F) (Z=0.4972, p-val=0.6191; Wilcoxon Ranksum test) The basic firing properties in IL. There are no significantly different between the PBS and MUS sessions.

2.3.2 The PL and IL cell activities were correlated with scene and choice information in the PBS session but decreased in the MUS session.

I constructed the cell firing rate map in sample-delay-response phases to see the firing rate difference among the scene trials. The left correct trials are in red(forest) and pink(city) color, and the right correct trials are in blue(city) and green(room) color in the firing rate map (left and right correct scenes were counterbalanced). Both the PL and IL showed scene-specific firing rate changes(Figure 16,17). In particular, the IL cells activity shows a scene-specific firing rate in the sample phase and a choice-specific firing rate in the delay phase (Figure 17). Also, these firing rate difference is larger than the PL. When the iHPC CA1 was inactivated, the task-specific correlation is disappeared in both regions. The results of these example cells show that the PL cells are correlated with the scene and choice information (Figure 18). In particular, the results show that the task-specific information maintenance in the IL and conversion from scene to choice information according to the phase (Figure 19). When the iHPC is inactivated, the correlation pattern of the PL and IL is disappeared. It indicates that the information from the iHPC to the mPFC is important for generating the task-specific firing pattern in the mPFC.

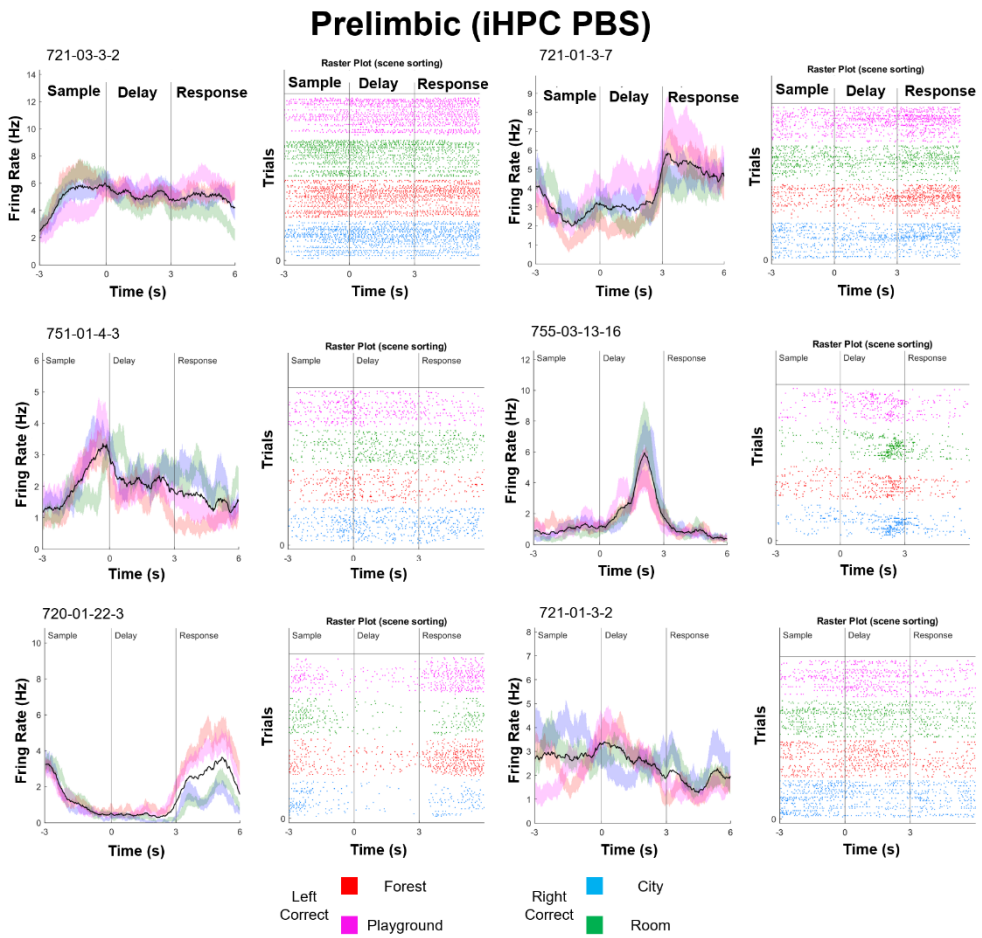

Figure 16. The PL cells show phase-specific firing rate differences in the sample-delay-response phases.

The left and right correct scenes are colored red-pink and blue-green. Black lines mean the average firing rate of total trials. The raster plots are shown on the right side of the rate map.

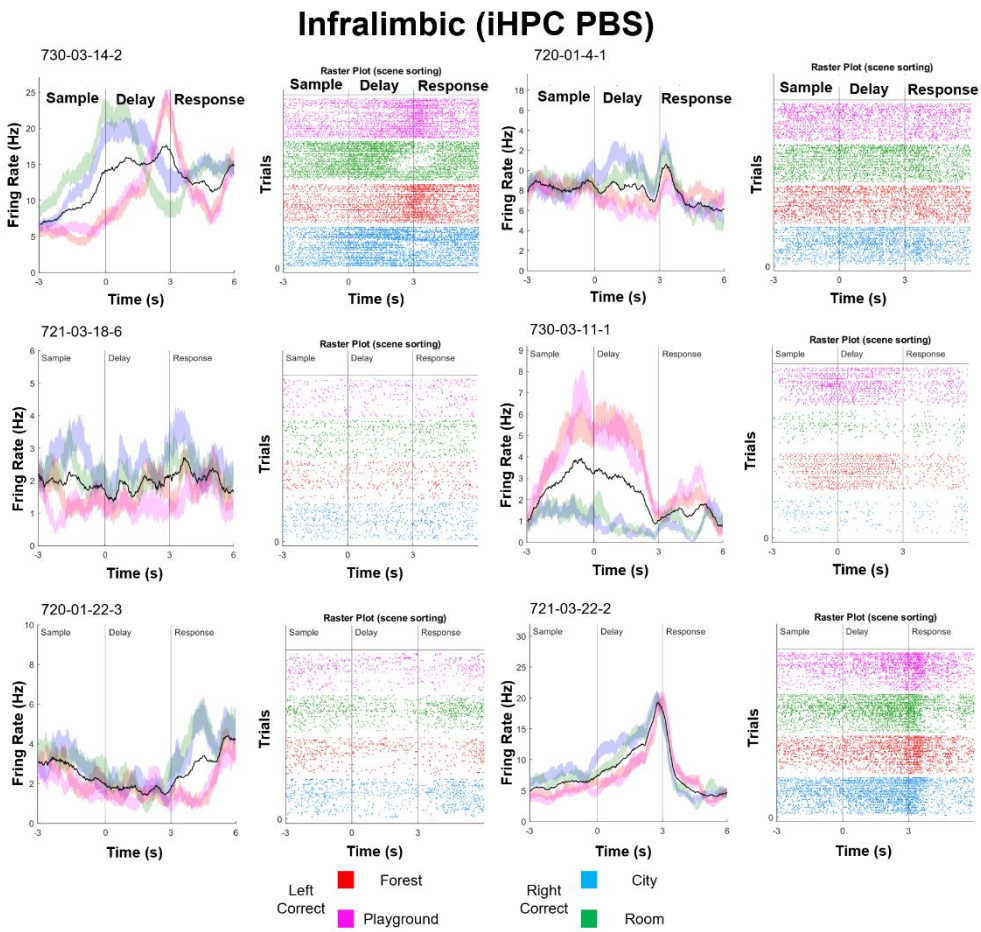

Figure 17. The examples of the IL cell show the task-relevant firing rate difference in all phases.

The firing rate difference in the IL between the left and right scene trials is larger than in the PL cells.

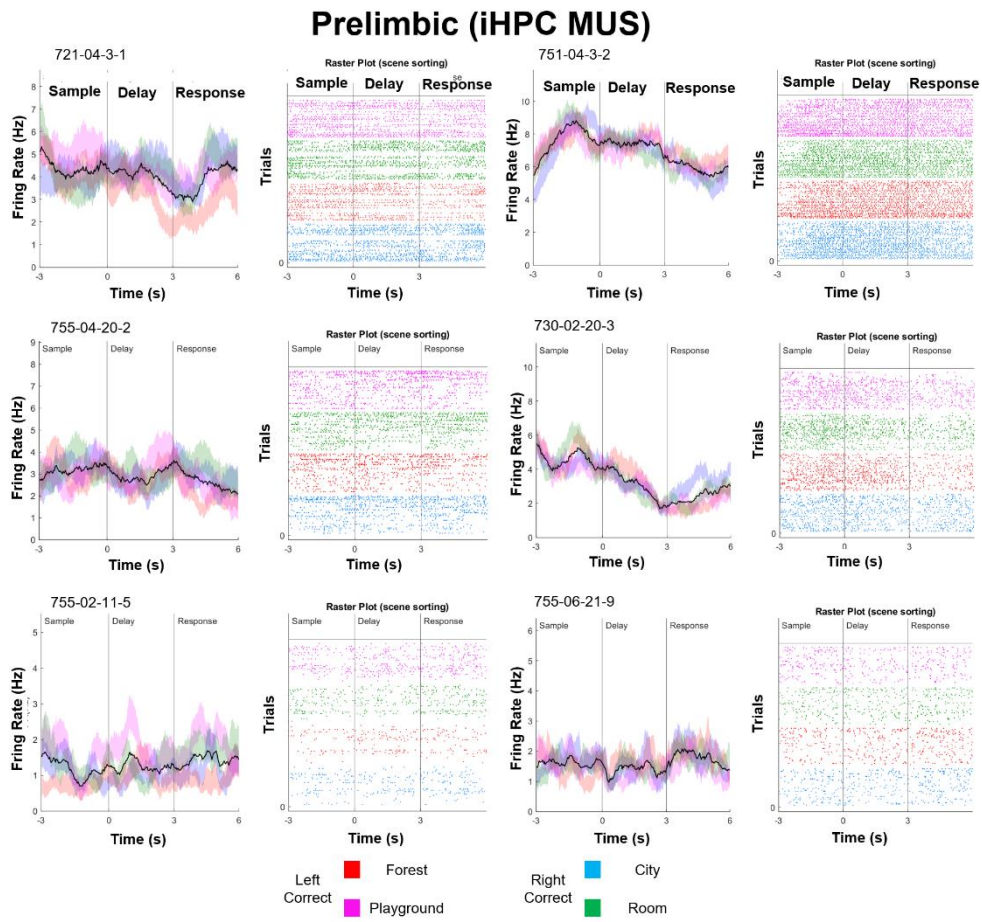

Figure 18. Firing rate differences disappear in the iHPC MUS session in the PL.

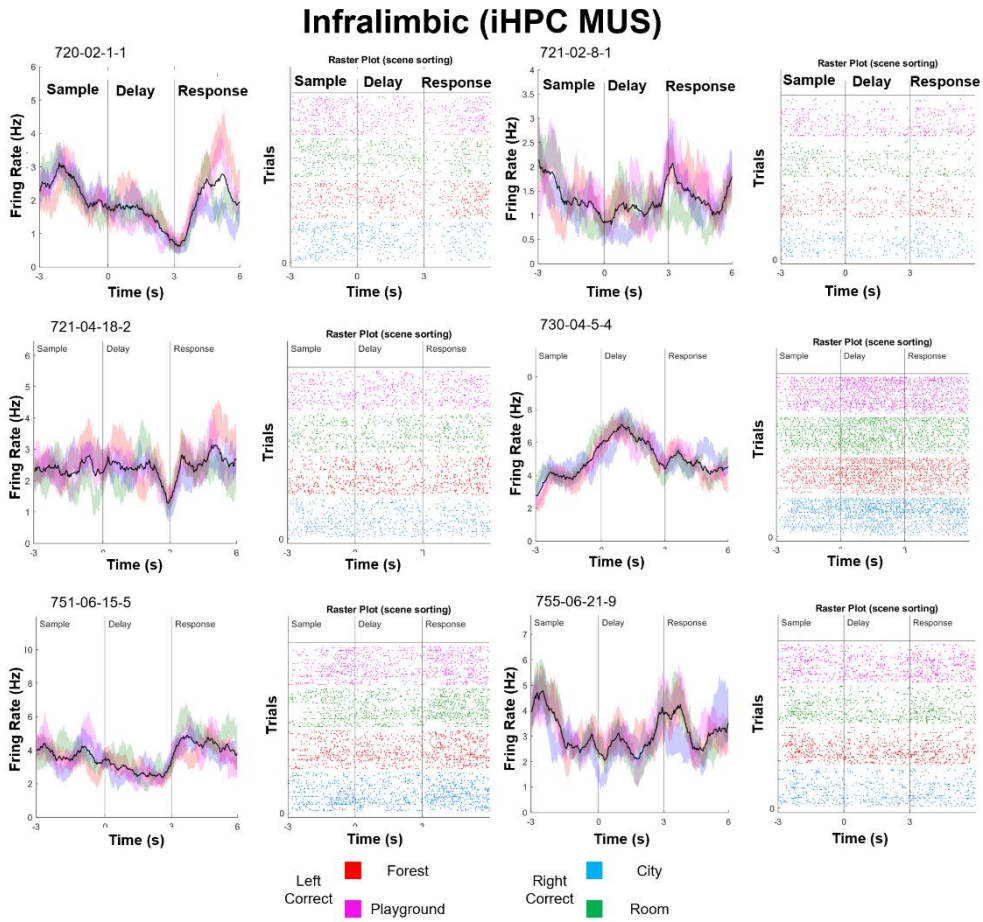

Figure 19. In the iHPC MUS session, the firing rate associated with the task demand is disrupted.

2.3.3 Phase-specific information in the PL and scene-associated choice information maintenance in the IL is disrupted with the iHPC inactivation

RDI was calculated to quantify the difference in rate for each scene and choice. When the iHPC was inactivated, the difference in RDI values with the PBS session in PL was examined. It shows that the RDIscn value significantly decreased in the sample phase ($Z=2.8923$, $p-val<0.01$, Wilcoxon ranksum test), and the RDIchc value significantly decreased in the delay phase ($Z=2.5034$, $p-val<0.05$, Wilcoxon ranksum test) (Figure 20,21). In these results, the iHPC to the PL circuit is important for processing the necessary information for each phase.

In the IL cells, the RDIscn value is significantly reduced in the response phase compared with the sample and delay phase ($X^2_{(2)}=11.19$, $p-val<0.01$, Kruskal Wallis test, Follows are post-hoc results by Wilcoxon Ranksum test with Bonferroni Correction. $\alpha=0.016$; Sample vs. Delay: $Z=0.3797$, $p-val=0.7$; Sample vs. Response: $Z=2.7182$, $p-val<0.01$; Delay vs. Response: $Z=3.048$, $p-val<0.01$). However, the RDIchc value is not a significant difference in all phases ($X^2_{(2)}=5.22$, $p-val=0.0734$, Kruskal Wallis test). These results indicate that the IL cells maintain the choice information in all phases. When the iHPC is inactivated, the RDIscn information is decreased in the sample phase ($Z=3.0682$, $p-val<0.01$, Wilcoxon ranksum test), and the RDIchc information is decreased in all phases(Sample: $Z=3.6344$, $p-val<0.001$, Delay: $Z=4.0505$, $p-val<0.001$, Response: $Z=3.0104$, $p-val<0.01$ Wilcoxon ranksum test)

(Figure 22,23). These results indicate that the iHPC is important for the scene-associated choice information and maintaining until the response in the IL.

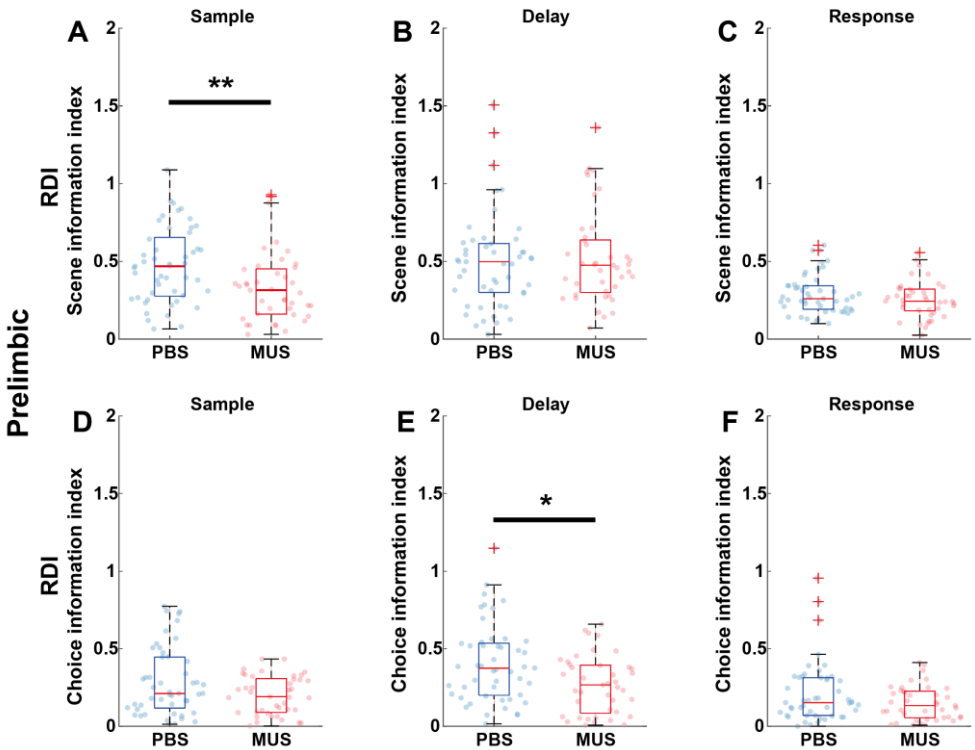

Figure 20. Box plot of the firing rate difference in the Prelimbic cortex. (A) In the sample phase, the rate difference between the scene trials. Blue dots mean the value of each cell. The blue colored box plot means the median value of the rate difference index in the PBS session. The Red box means the median value of the rate difference index in the MUS session. (B) Same as the (A) but in the delay phase. (C, Same as the (A) but in the response phase.

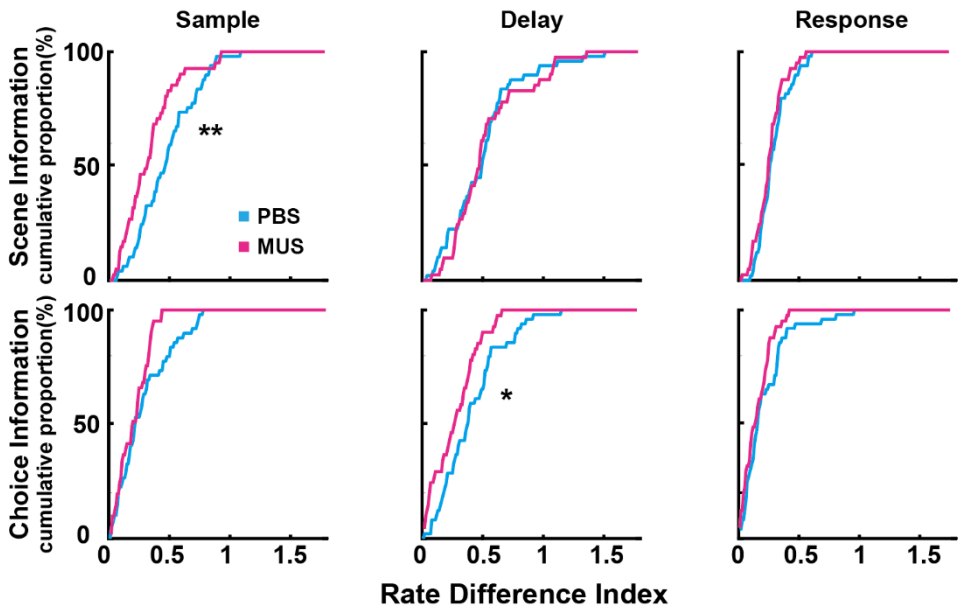

Figure 21. The scene information in the sample phase and the choice information in the delay phase are significantly decreased with the iHPC inactivation in the PL.

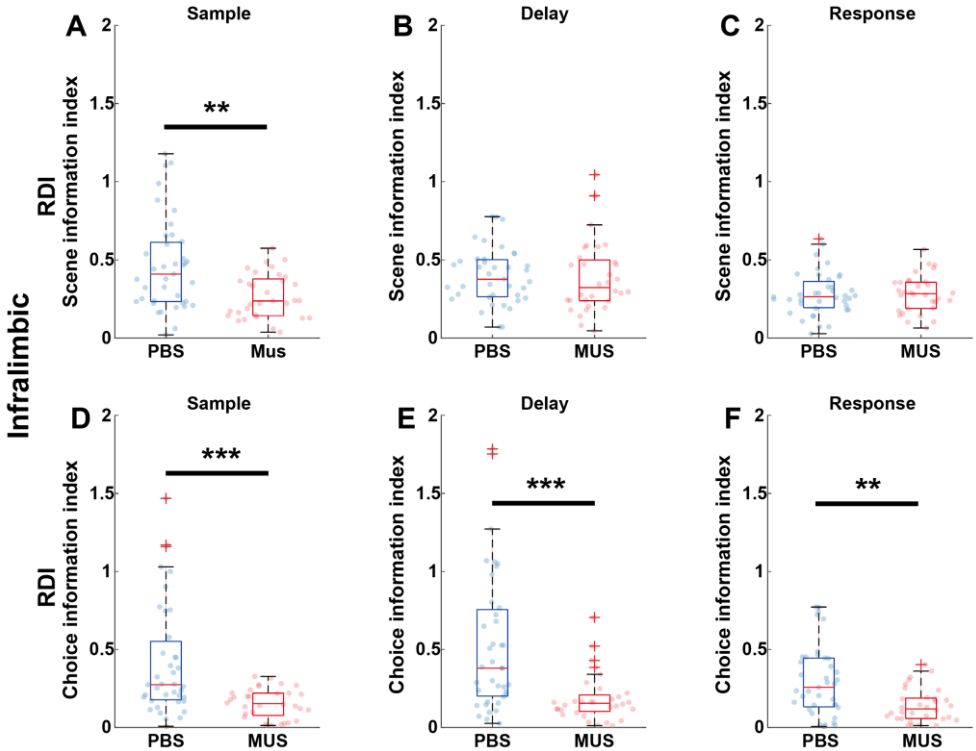

Figure 22. Box plot of the firing rate difference in the Infralimbic cortex.

(A)(D) In the sample phase, the scene and choice information is significantly decreased. (B)(E) In the delay phase, the choice information is significantly decreased between the PBS and MUS session. (C)(F) In the choice phase, the choice information is disrupted in the MUS session.

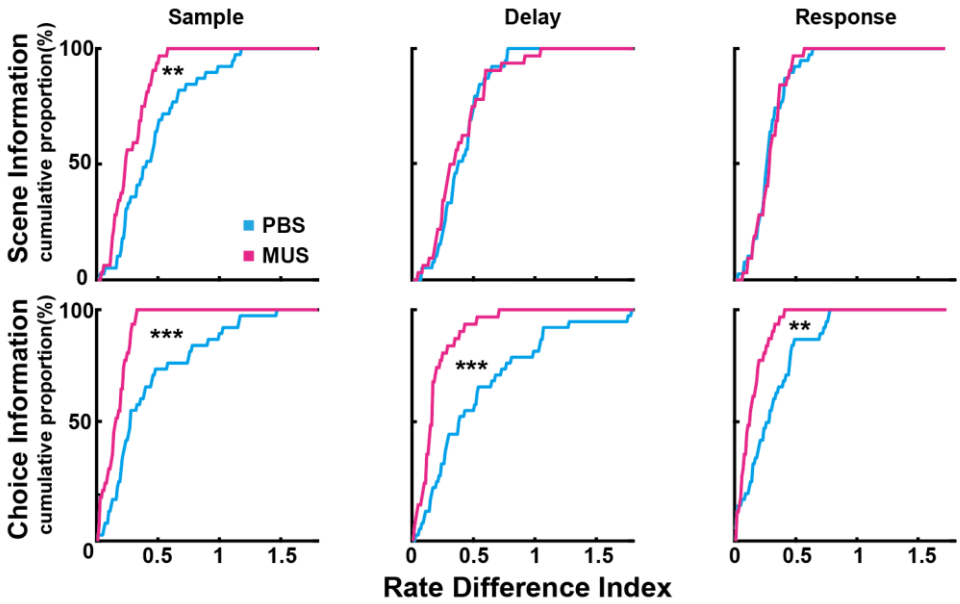

Figure 23. The scene information is significantly decreased only in the sample phase. On the other hand, the choice information is significantly decreased in all phases with the iHPC inactivation in the IL.

2.3.4 The choice information is significantly decreased in the delay phase in the IL.

In the sample phase, the scene information is significantly decreased in the PL and IL. However, the choice information is significantly decreased in the IL but not in the PL. Notably, the decreasing rate of the choice information in the delay phase in the IL is larger than in the PL. These results indicate that the choice information maintenance is critical between the iHPC and IL area, but in the PL, this information processing strength is weakened in the delay phase than in the IL. The choice information in the IL mostly disappears in all phases, but in the PL, the choice information only decreased in the delay phase (Figure 24).

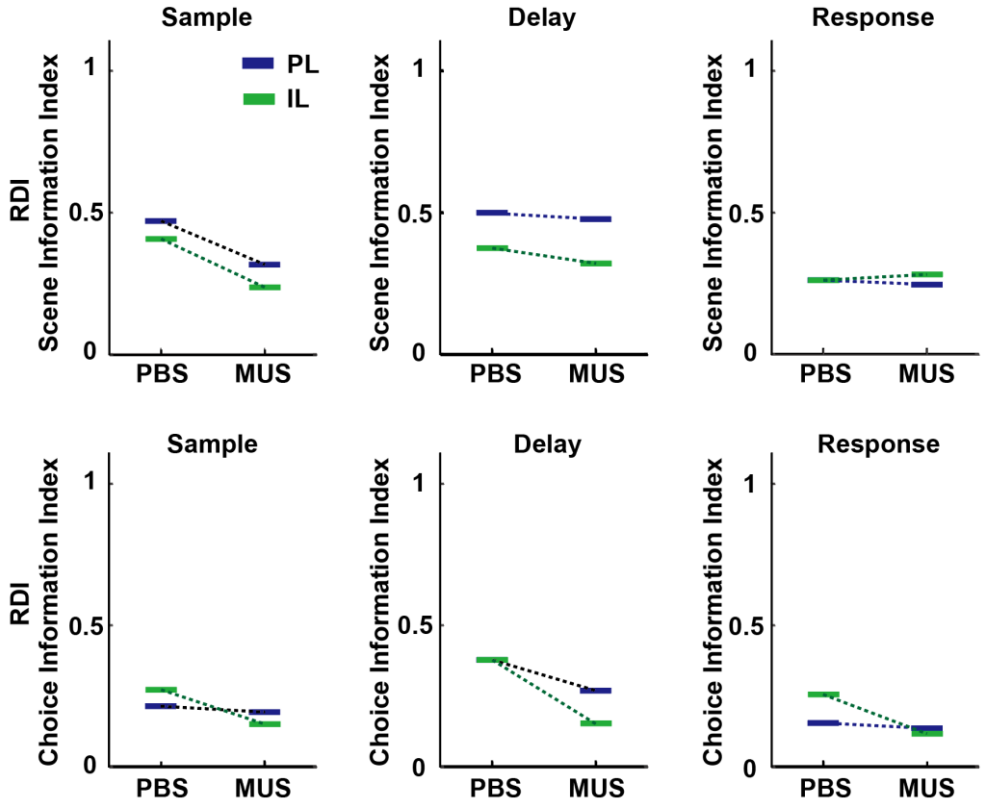

Figure 24. The difference between the PBS and MUS session in the IL is more prominent than in the PL.

In the median value of the PBS and MUS session in each phase, the difference between the PBS and MUS session. Especially in the delay phase, the choice information is significantly decreased in the MUS session in the IL. The choice information is also decreased in the delay phase but not as large than the delay phase.

2.3.5 The dynamic shift of neural correlates between sample and delay phases in the IL decreased with the iHPC inactivation

I found that the scene-associated choice information-specific firing cells changed their information to the choice information from the sample to the delay phase in the IL (Figure 25). In the flow chart, the proportion of scene-specific cells is presented in red color, the choice-specific cell is presented in blue color, and both scene and choice-specific cells are presented in purple color. Notably, the majority of cells from the sample to the delay phase in the IL changed their information scene-associated choice information to the choice information. I calculate the rate difference index in all phases to track the cell information from the sample to the response phases. To simultaneously compare the RDIscn with the RDIchc in a cell, I obtained the 2D plot, which consisted of the x-axis as the RDIscn value and the y-axis as the RDIchc value (Figure 26). The IL and PL cells are plotted on the 2D space by dividing the phase. Especially, the IL cells dynamically shift to the RDIchc side in the delay phase (Figure 26B) but not in the PL cells (Figure 26A). I calculated the angle value (tanθ), if the tanθ of the cell is larger than 0.79 it means the cell process the choice information more than the scene information. On the contrary, if the tanθ is smaller than 0.79, it indicates that the cell conveys the scene information more than the choice information (Figure 27). In the delay phase, the fitting line on the histogram shows that cells in the IL change their information from the scene information to the choice information (Figure 28). However, if the iHPC is inactivated, the information change disappears in the

delay phase. In order to track the angle of each cell according to the phase, the tanθ of the sample phase was subtracted from the tanθ of the delay phase(Δtanθ) also the delay phase was subtracted from the response phase. The Δtanθ is significantly different in the sample-delay phase in IL cells ($Z=2.0859$, $p-val<0.05$, Wilcoxon Ranksum test) (Figure 29B), but not different in the iHPC MUS session. There are no significant differences in the PL cells in all phases (Figure 29A). These results indicate that the dynamic shift of neural correlates between sample and delay phases shows in the IL cells, and the iHPC plays an important role in the flexible change of the information in the IL.

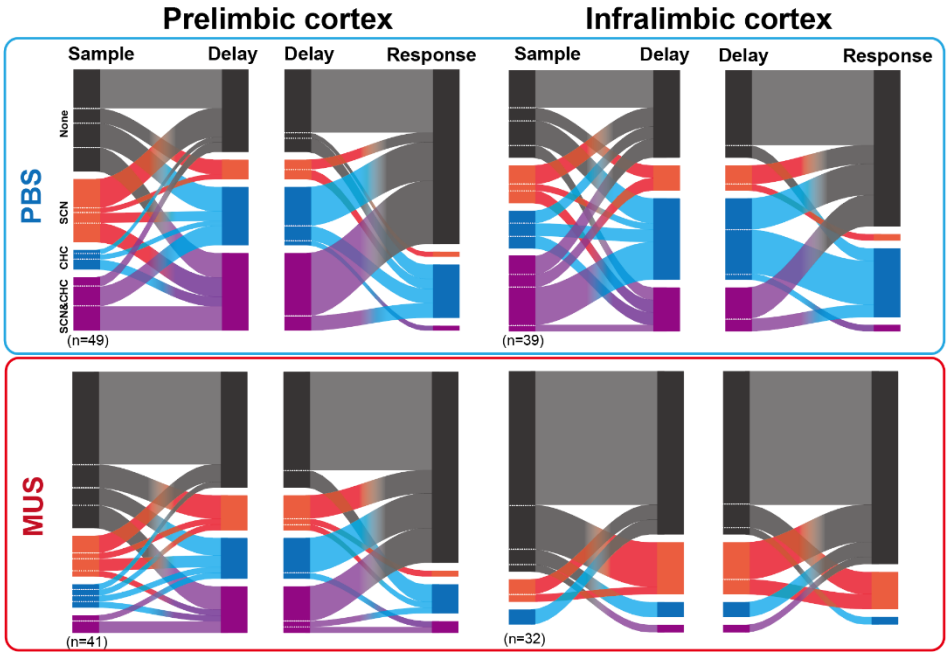

Figure 25. Task-specific information flow in the sample-delay-response phases

In the sample-to-delay phase, the scene-associated choice information (purple) is shifted to the choice information (blue). Also, the choice information is maintained from the delay to the response phase (blue).

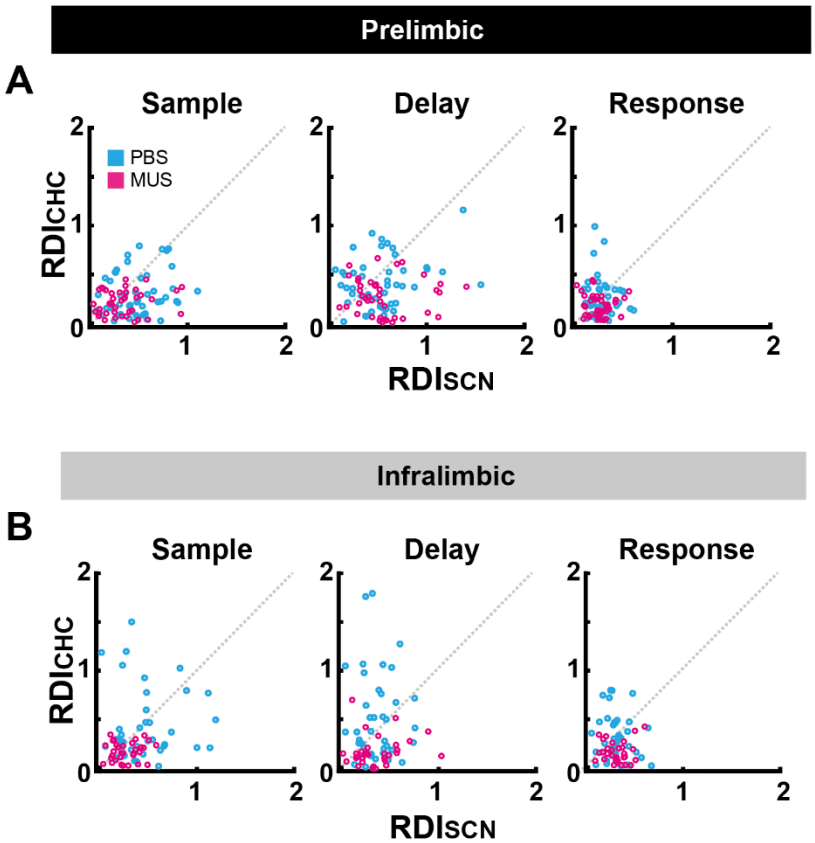

Figure 26. The IL cells shifted their information from scene to choice in the sample-delay phases.

(A) The PL cells are not shown the shifting their information through the sample to the response phases. And the pattern between the PBS and MUS sessions is not different. (B) The IL cell positions are shifted above the diagonal in the delay phase. However, this movement is not shown in the MUS session.

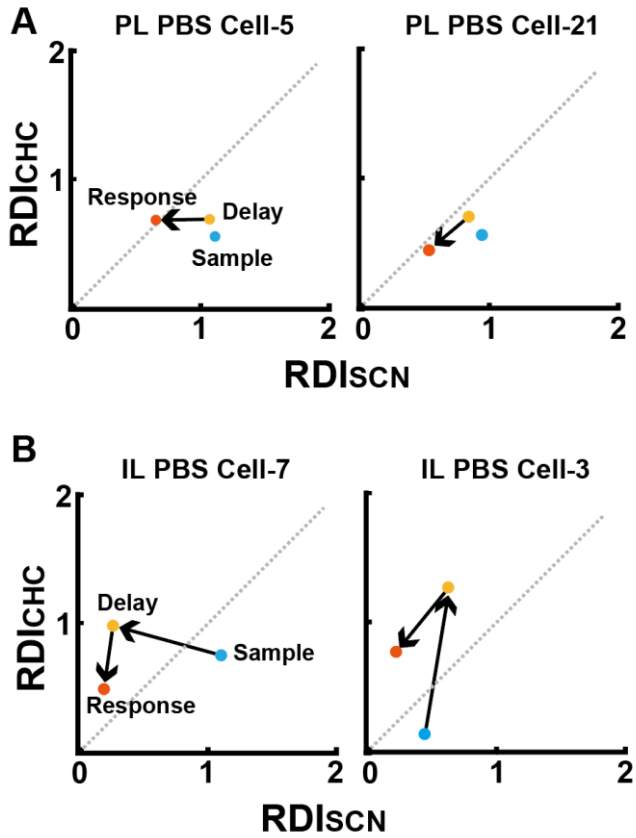

Figure 27. Single cell examples in sample-delay-response phases. (A) The PL cell examples. The position of the cell in the sample to delay phase does not shift. (B) The IL cell examples. In the sample phase, the cells are positioned below the diagonal, but in the delay phase, the cells are positioned above the diagonal.

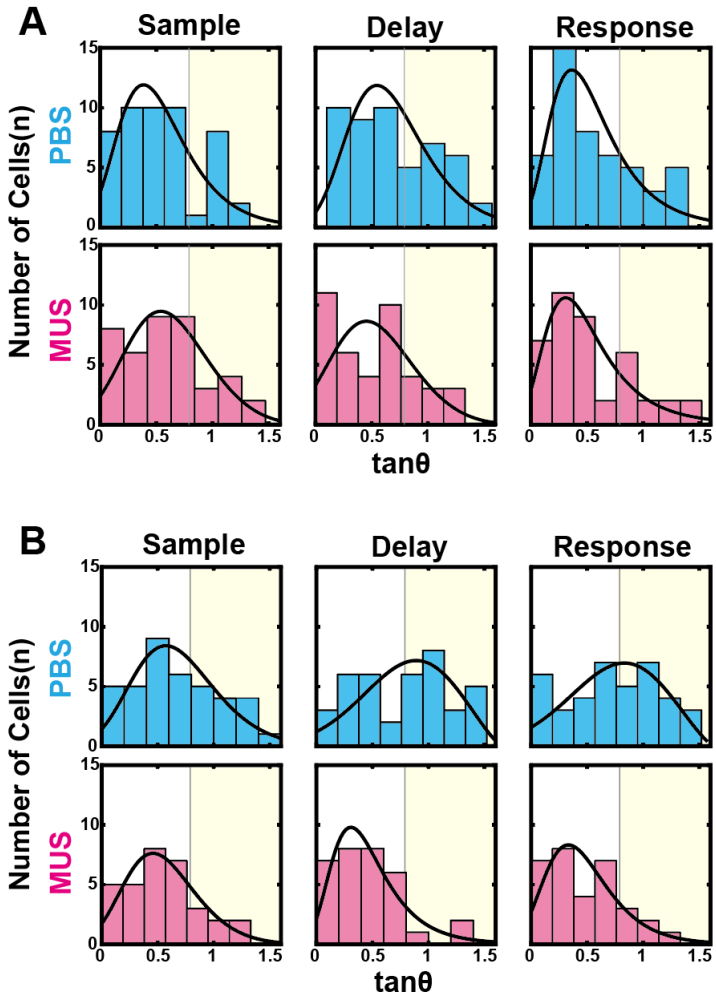

Figure 28. The angle value is increased in the delay phase in the IL but this pattern is disappeared in the MUS session.

(A) The histogram of the angle value in the PL. The angle value of the cells is not increased in the delay phase. (B) The histogram of the angle value in the IL. In the PBS session, the fitting line verges to the right side in the delay phase, but this pattern is disappeared in the MUS session.

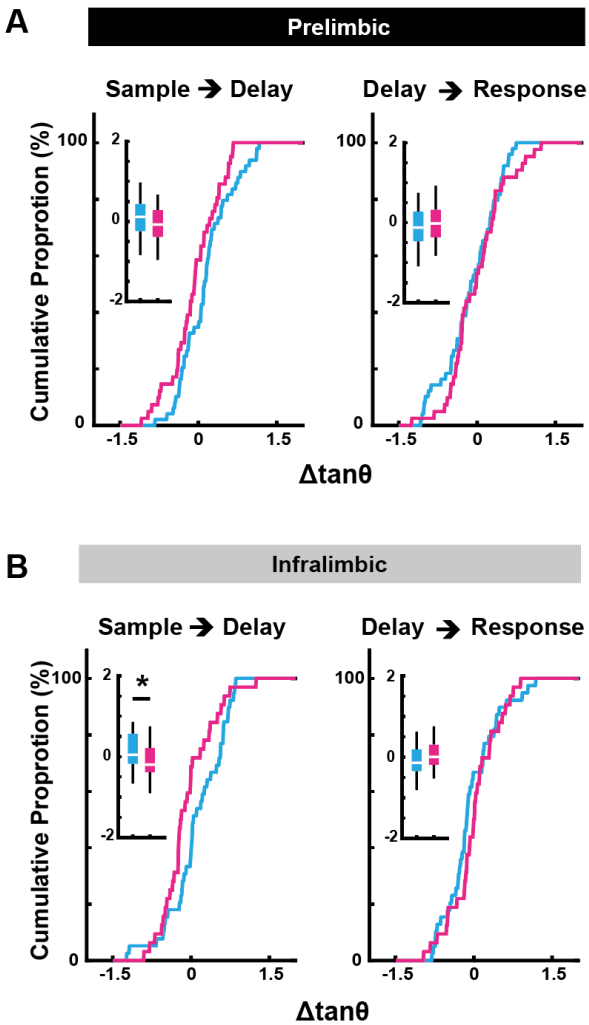

Figure 29. The angle value change between the phases is significantly different from the sample to the delay phase in the IL cells.

(A) The Δtanθ(difference in angle) is no difference between the PBS and MUS session in the PL cells. (B) The Δtanθ is significantly different in the PBS and MUS sessions in the IL cells between the sample and delay phases.

2.4 Discussion

In the current study, the iHPC-IL network plays an important role in the working memory task. The PL also conveys task-relevant information, but the effect of the iHPC inactivation is smaller than the IL. The IL cells dynamically change their scene-associated choice information to the choice information in the delay phase to appropriate action according to the environment. However, the PL cells do not show the information changing in the delay phase. When the iHPC is inactivated, the information changing in the IL is disrupted. This result indicates that the iHPC to IL network is critical for flexibly changing their information according to the phase. The place-associated value information is likely projected from the iHPC, and the results from this study indicate that the iHPC-IL network maintains the choice information during the delay phase to get a goal. To verify whether the iHPC and IL network are strengthened in the working memory task phase, I calculated the theta power and the theta phase locked cell proportion in the IL and PL in chapter 3.

Chapter 3

3.1 Introduction

The coherence of theta (4–12 Hz) is one of the important communication methods of the HPC and PFC. According to previous papers, the HPC and PFC in rats performing working memory tasks showed coherence of the phase in the delay–choice period (Siapas et al., 2005). In addition, the PFC cells were phase–locked of the HPC was found(O'Neill et al., 2013). Based on the coherence and phase–locking population results of the two regions, the theta is an important network operation mechanism. When the vHPC is inactivated, the theta power of the mPFC is not different, but the theta coherence of the dHPC and mPFC decreases. These results show that the vHPC is important for communication between the HPC and mPFC. However, the function of theta is not verified in the scene–based working memory task between the HPC and mPFC yet. I verified whether these phenomena also appear when the rat performs scene–based working memory tasks.

3.2 Materials and Methods

3.2.1 Tetrode selection

To align and eliminate the baseline offsets, local field potentials (LFP) were down-sampled from 32kHz to 2kHz with a 3-300 Hz zero-phase bandpass filter (Butterworth filter, "filtfilt" function in MATLAB). The power spectral density (PSD) function was obtained using the Chronux ToolBox (MATLAB). And then, the reference tetrode with the highest power for individual sessions and regions was selected to analyze the spiking associated with the theta rhythm.

3.2.2 Theta phase-locking strength

The preferred phase of the cell spike in the theta(4-12 Hz) phase was investigated to verify the relationship between the single-cell activity and the LFP. The LFP of the mPFC was filtered in the theta range using a third-order zero-phase Butterworth filter. To quantify the strength of the single-cell spiking activity paired with phase-locking to the theta wave, I calculated the mean resultant length(MRL; Circular Statistics Toolbox; MATLAB) of each spike-LFP pair (n = 49 in the PL PBS, n=41 in the PL MUS, n=39 in the IL PBS and n=32 in the IL MUS). The MRL value represents the consistency level between the spike time of a cell and the LFP oscillation. To determine the significance of the phase-locking strength I calculate the p-value using Rayleigh' s test. (Ahn et al., 2019). I only use the sessions with speeds is 5cm/s to 30cm/s to control the speed issue.

3.2.3 Statistical analysis

There are 4 sample scenes and two lick port choices in the behavior paradigm in the scene-based working memory task. To verify the cell has significant information about the scene or choice or both information, I calculate the mean firing rate in each scene and choice trial. After that, the mean firing rate of each scene trial is compared with the Kruskal-Wallis test (1-way ANOVA test), and the choice trial is compared with the Willcoxon Ranksum test in MATLAB. If the cell has a p-value<0.05 in the Kruskal-Wallis test, it is determined to have a significant value in scene information. If the cell has a p-value<0.05 in the Ranksum test, it is determined to have a significant value in choice information.

3.3 Results

3.3.1 Theta Power is increased in the IL in the delay phase and this pattern is disappeared when the iHPC is inactivated

Theta power is calculated in the sample and delay phases (Figure 30). To eliminate the alternative hypothesis about the behavioral difference in animals between the sample and delay phases, I calculated the speed of each session and excepted the sessions if the speed was lower than 5cm/s. After the exception, there are 6 sessions left in the PBS session, 7 sessions left in the MUS session. In the IL, theta power is increased in the delay phase compared with the sample phase (Figure 31). However, in the PL, there is no difference in theta power between the sample and delay phases (Figure 31). When the iHPC is inactivated, the difference in the power between the sample and delay phases are disappeared in the theta frequency in the IL (Figure 32). There is a slight difference between the sample and delay phase in the PL, but this difference is not statistically significant (Figure 32). For each tetrode, theta power is calculated. There is a significant difference in the theta power between the sample and delay phases in the IL but not in the PL in the iHPC PBS session. A one-way repeated-measures ANOVA showed a significant effect of phase in the IL($F=13.003$, p-value<0.001); but not in the PL ($F=1.538$, p-value$=0.2338$) (Figure 33). In the IL, there is a significant difference in power between the sample and delay phase (p-value<0.01; Bonferroni-Dunn), also between the delay and ITI phase (p-value<0.0001; Bonferroni-Dunn)

(Figure 33). However, in the iHPC MUS session, there is disappeared the power difference between the sample and delay phases in the IL (F=6.267, p-value=0.0114; one-way ANOVA), (p-value=0.0435; Bonferroni-Dunn)(Figure 34). The speed in the delay phase is slightly lower than the sample phase but not significantly different statistically (Figure 35). These results indicate that the projection from the iHPC has more effect on the IL than the PL in the delay phase of the scene-based working memory task.

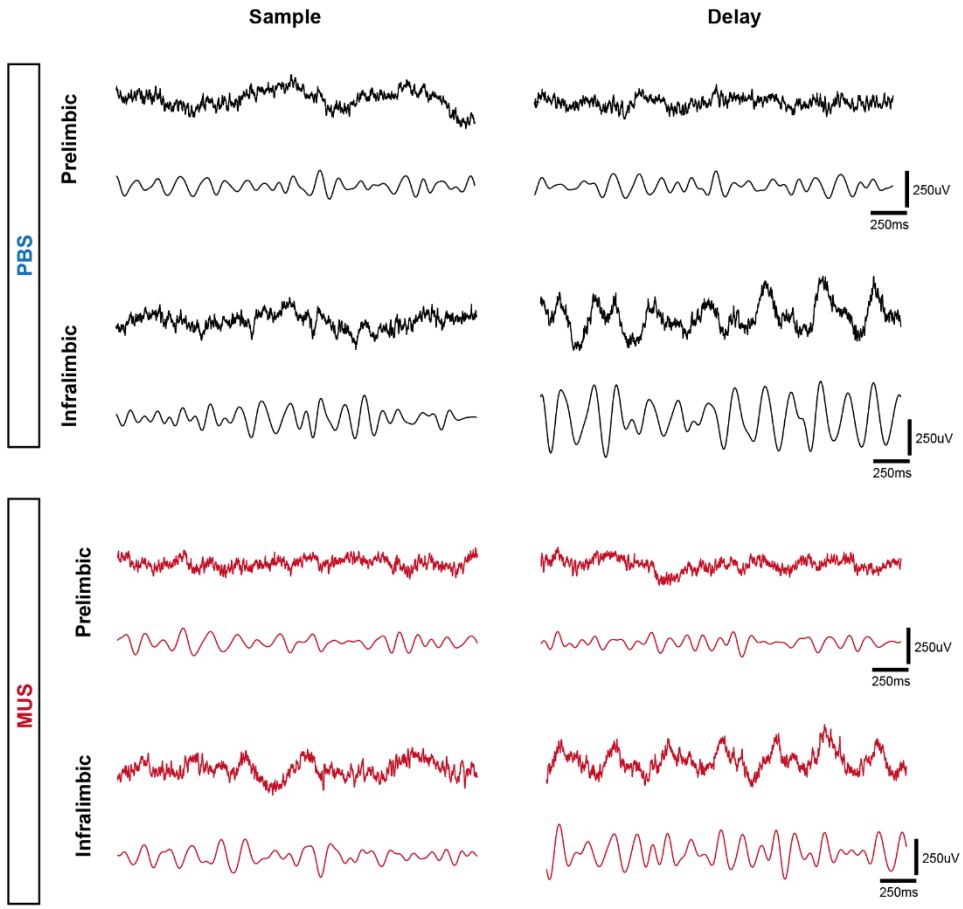

Figure 30. The representative examples of theta wave in the PL and IL

In the IL, the theta power is increased in the delay phase compared to the sample phase. In the PL, there is no difference in theta power between the sample and delay phases (black lines). However, in the MUS session (red lines), Theta power is similar between the sample and delay phases.

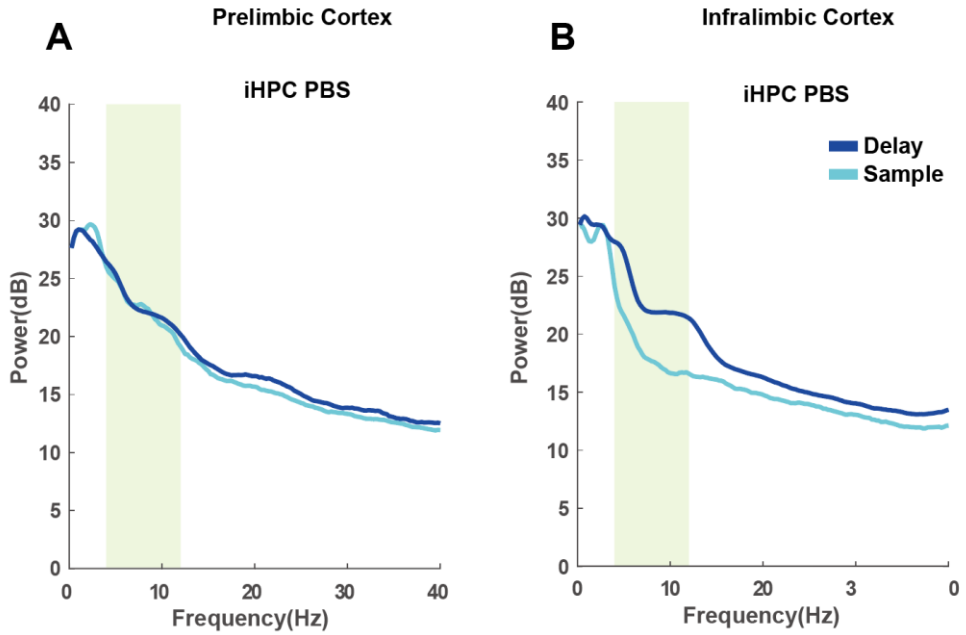

Figure 31. Theta power in the IL is significantly increased in the delay phase.

(A) In the IL, the theta(green area) power is increased in the delay phase compared to the sample phase. (B) In the PL, there is no difference in theta power between the sample and delay phases. The Cyan line means the sample phase, and the Blue line means the delay phase.

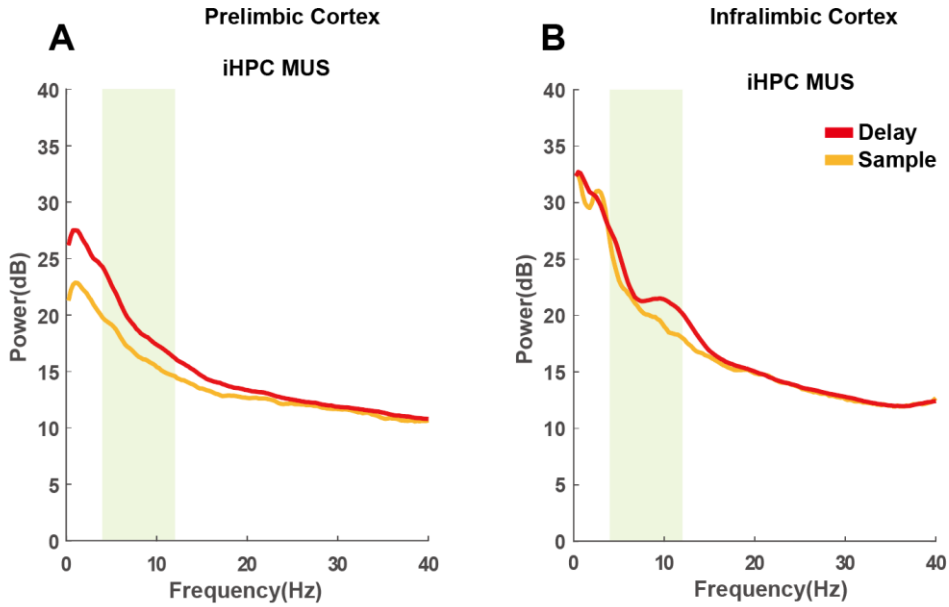

Figure 32. When the iHPC is inactivated, theta power in the IL is not increased.

(A) In the IL, the theta(green area) power is not increased in the delay phase compared to the sample phase when the iHPC is inactivated. (B) In the PL, there is no difference in theta power between the sample and delay phases. The yellow line means the sample phase, and the Red line means the delay phase.

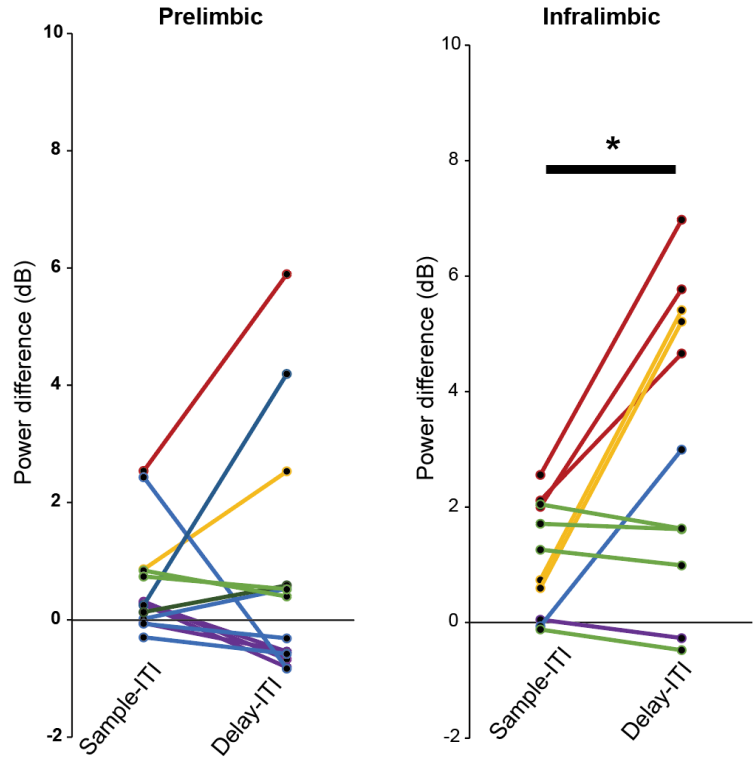

Figure 33. Theta power is significantly increased in the delay phase in the IL but not in the PL.

(A) Theta power is significantly increased in the delay phase. Gray lines indicate each cell's theta power. The Red line indicates the mean theta power. (B) Same as the (A) but in the PL. Theta power is not increased in the PL. Different Colors mean different sessions.

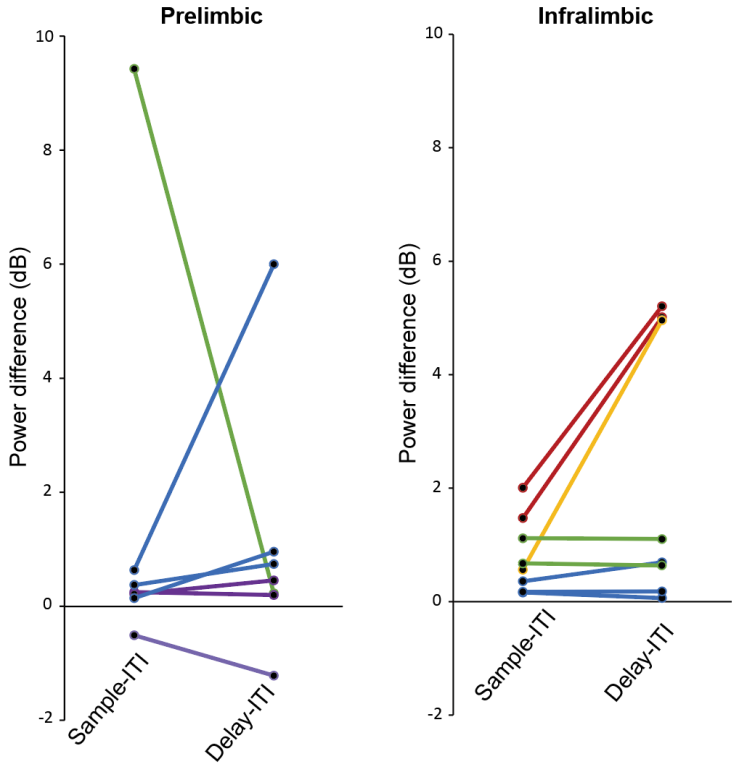

Figure 34. Theta power is not increased in the delay phase when the iHPC is inactivated.

(A) The pattern of difference between the sample and delay phases disappears in the iHPC MUS session. (B) There is no significant increase in theta power in the PL. Different Colors mean different sessions.

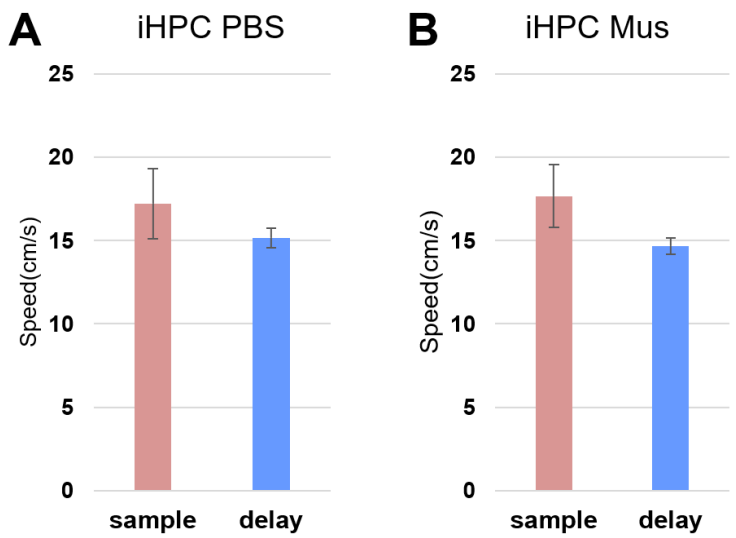

Figure 35. The speed is not different between the sample and delay phases.

(A) The speed in the sample and delay phase are not different in the PBS session. (B) Also, the speed in the sample and delay phases are not different in the MUS session.

3.3.2 The strength of the theta phase-locked cell in the delay phase is significantly larger than the sample phase.

The mean resultant length (MRL) of the sample and delay phases was calculated to verify whether the cell showing the preferred phase according to the scene maintains phase-locking strength in the sample and delay phase (Figure 36,37). The MRL value is increased in the delay phase in the PBS session in the PL (DF=19, p-value<0.01, paired t-test) (Figure 38A). The MRL value is significantly increased in the delay phase compared to the sample phase in the PBS session (DF=15, p-value<0.01, paired t-test) (Figure 38C). In the MUS session, the difference between the sample and delay phases is not shown (Figure 38B,D). The MRL value and spike number difference between the sample and delay phases are not shown a positive correlation (Figure 39). These results indicate that the iHPC plays a critical role in theta phase-locking in the delay phase in the PL and IL.

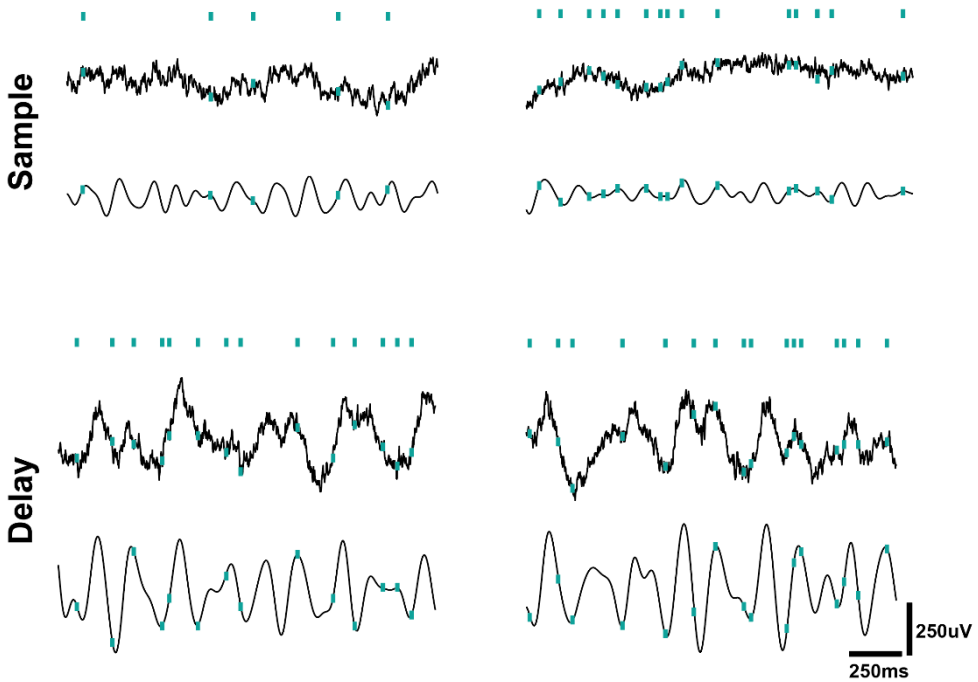

Figure 36. Representative theta phase and the spiking activities in the sample and delay phase.

The blue bars are the individual cell spiking activities. The black lines are the raw LFP trace(upper) and filtered LFP in the theta range(under). In this example, the spikes are mostly positioned on the trough of the theta cycle in the delay phase.

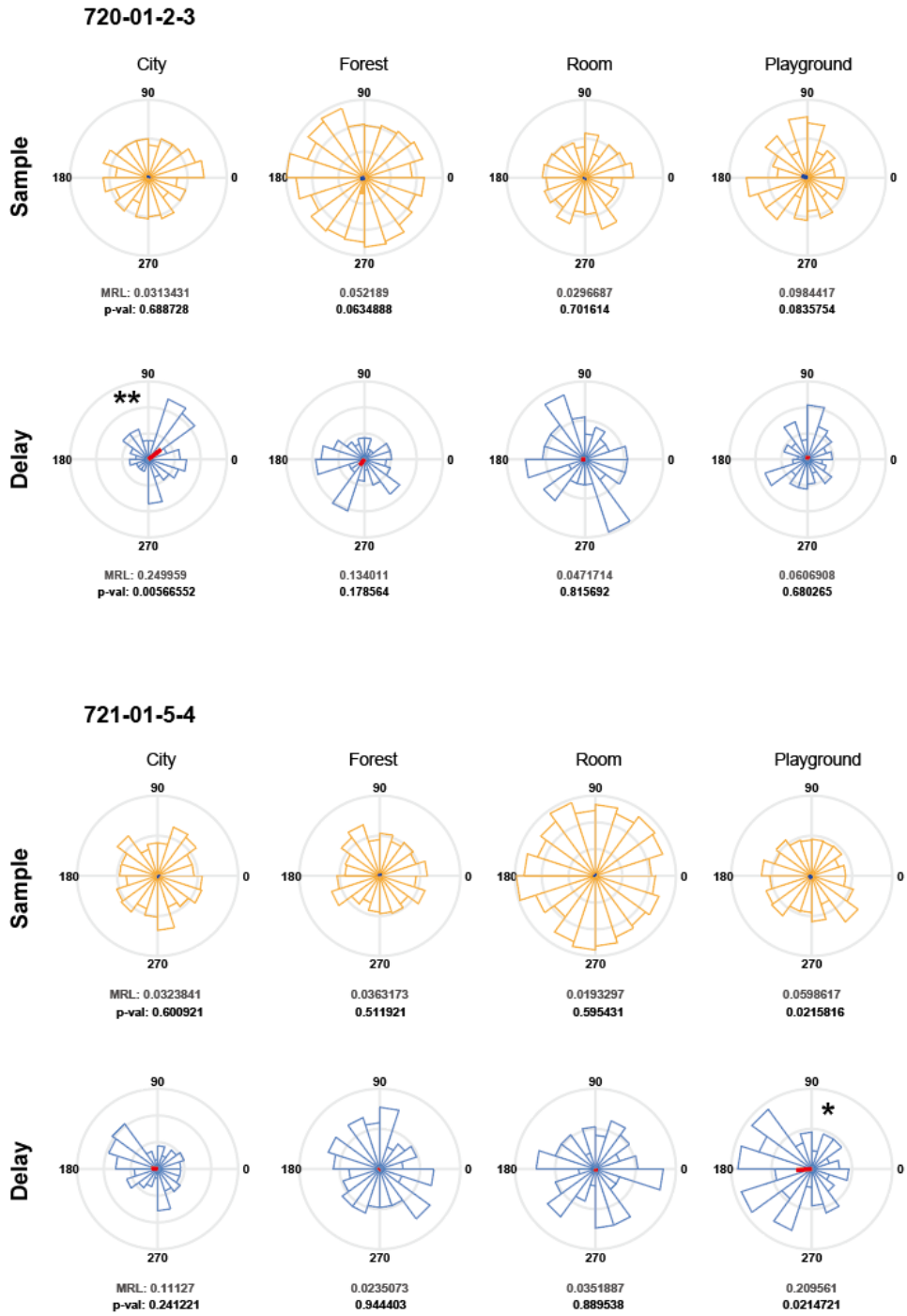

Figure 37. Theta phase-locking strength is increased in the delay phase than in the sample phase.

The examples of the preferred phase in each scene trial. The MRL value in the delay phase is larger than in the sample phase.

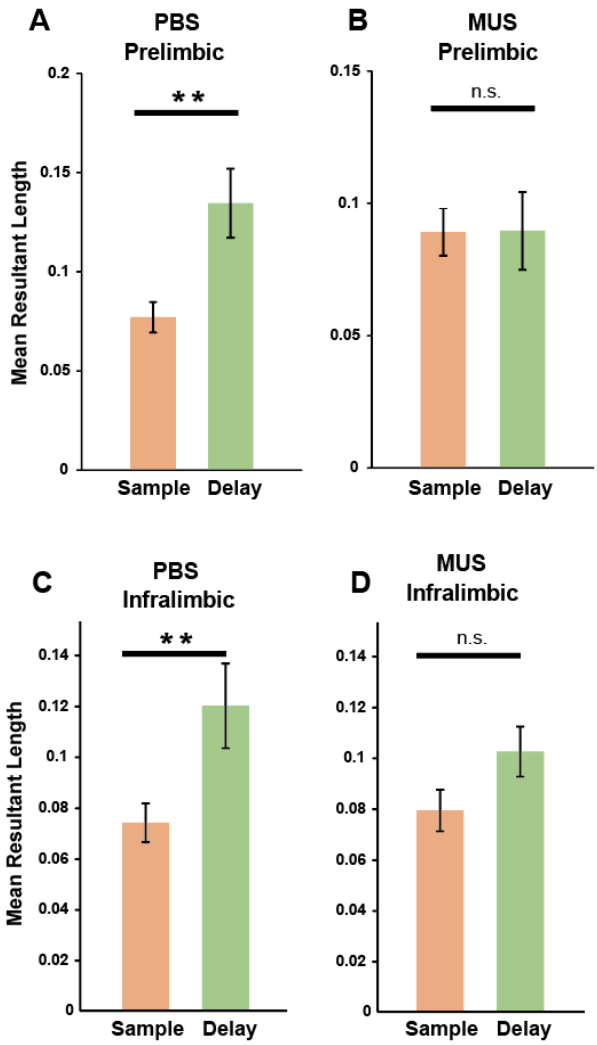

Figure 38. The phase-locking strength increases significantly in the delay phase but disappears in the MUS session.

(A) The MRL value is significantly increased in the delay phase in the PL. (B) However, in the MUS session, the MRL value between the sample and delay phases are similar. (C) Same as the (A) but in the IL. (D) Same as the (B) but in the IL.

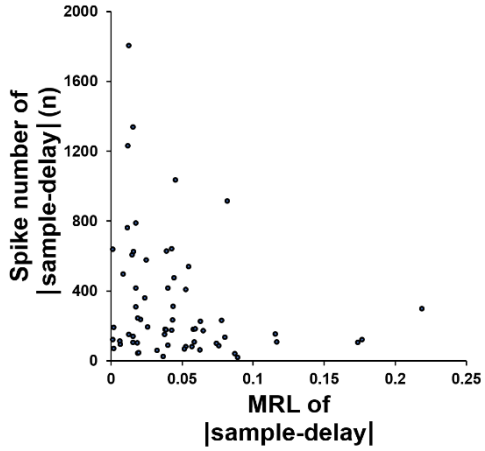

Figure 39. There is no positive correlation between the spike number and MRL value difference between the sample and delay phase.

3.3.3 The IL cell activities were mainly correlated with choice information in the PBS session but decreased in the MUS session in the delay phase.

In the results of the theta phase analysis, it was found that the delay phase is the most affected by the iHPC-IL circuit in the working memory task. Therefore, I focused on the delay phase to find what information is projected from the iHPC to the IL. The proportion of the task-relevant cells in the IL is about 50%, but this proportion is significantly decreasing in the MUS session in the delay phase($X^2(2)=11.3917$, p-value<0.01, Chi-square test). Most cells are correlated with the choice information, and this correlation is decreased in the MUS session. However, in the PL, there is no difference in the proportion even after inactivating the iHPC (Figure

40). It indicates that the iHPC to IL projection in the delay phase is important for the working memory task but not for the PL.

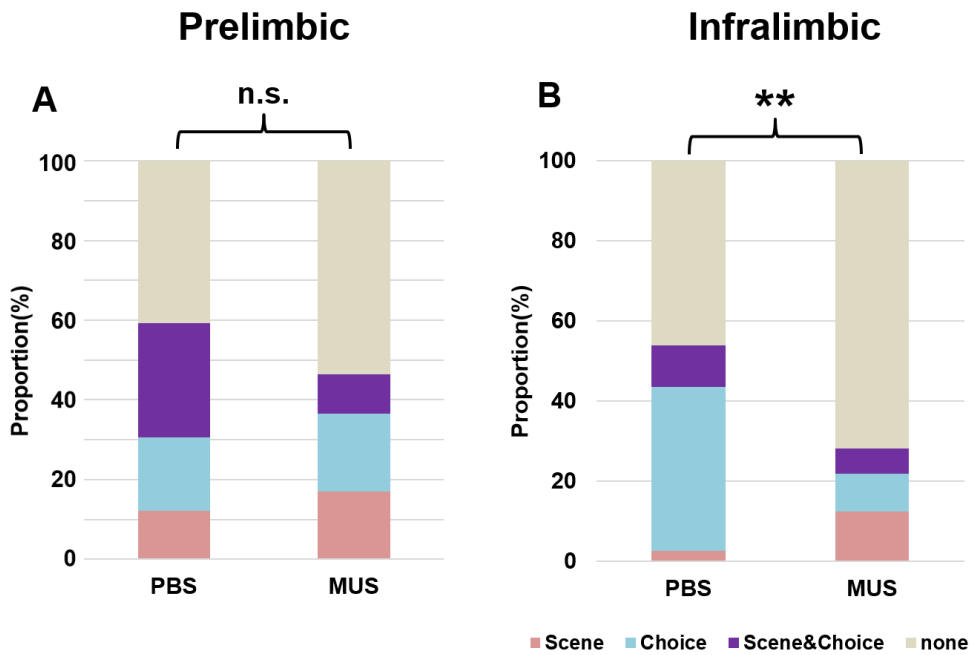

Figure 40. The IL cell activities were correlated with choice information in the PBS session but decreased in the MUS session.

In the IL, there is a significant difference in the proportion of the task-relative cells between the PBS and MUS sessions. However, in the PL, the proportion between the PBS and MUS sessions is similar.

3.3.4 The PL is related to the scene-associated choice information processing in the delay phase

In the PBS session, the proportion of theta phase-locked cell in the delay phase is 20.4%, and the non-locked cell is 79.6% (Figure 41A). Notably, theta phase-locked cells and non-phase-locked cells in the PL have scene and choice specificity (Figure 41B). In the MUS session, the proportion of theta phase-locked cells is 14.6%, and the non-locked cell is 81.3% (Figure 41C). The scene-specific cells disappear in the phase-locked cell population, and the scene-associated choice information cells disappear in the non-phase-locked cell population (Figure 41D). These results indicate that the non-phase-locked cells in the PL play important roles in scene and choice information processing in the delay phase. And the iHPC to PL projection is not related to the choice information processing.

3.3.5 The network of the iHPC to the IL is critical for the choice information processing

In the PBS session, the proportion of theta phase-locked cell in the delay phase is 25.6%, and the non-locked cell is 74.4% (Figure 42A). I contrast the phase-locked cells with the task-relevant information results to verify what information is processed in the phase-locked cells, which are considered to be directly affected by the iHPC. Surprisingly, theta phase-locked cells have only the choice information, but non-phase-locked cells have choice and scene information (Figure 42B). It indicates that iHPC to IL projection deals with the choice information in the delay phase for the appropriate

action in the response phase. In the MUS session, the proportion of theta phase-locked cells is 18.8%, and the non-locked cell is 81.3% (Figure 42C). Theta phase-locked cells in the MUS session might be affected by the theta of the dHPC. On the other hand, in the MUS session, phase-locked cells have only the scene information (Figure 42D). Because the iHPC is inactivated, there is no value information from the dHPC. For this reason, the mPFC can not shift from the scene information to the choice information in the delay phase. These results show that the circuit from the iHPC to the IL is critical for the choice information processing in preparation for the response phase after the delay.

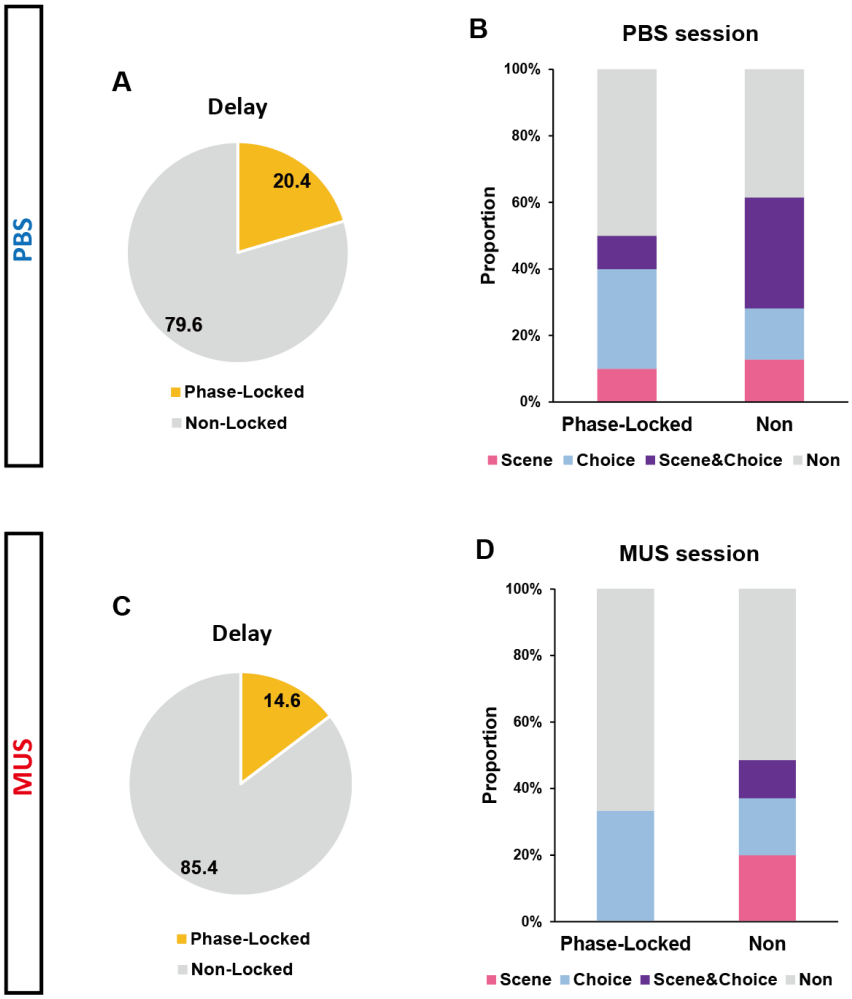

Figure 41. Theta phase-locked cells convey the scene and choice information in the PL.

Theta phase-locked cells in the PL carry the scene and choice information in the delay phase. Non-locked cells also have both choice and scene information. In the MUS session, the scene information is disappeared in the theta phase-locked cells.

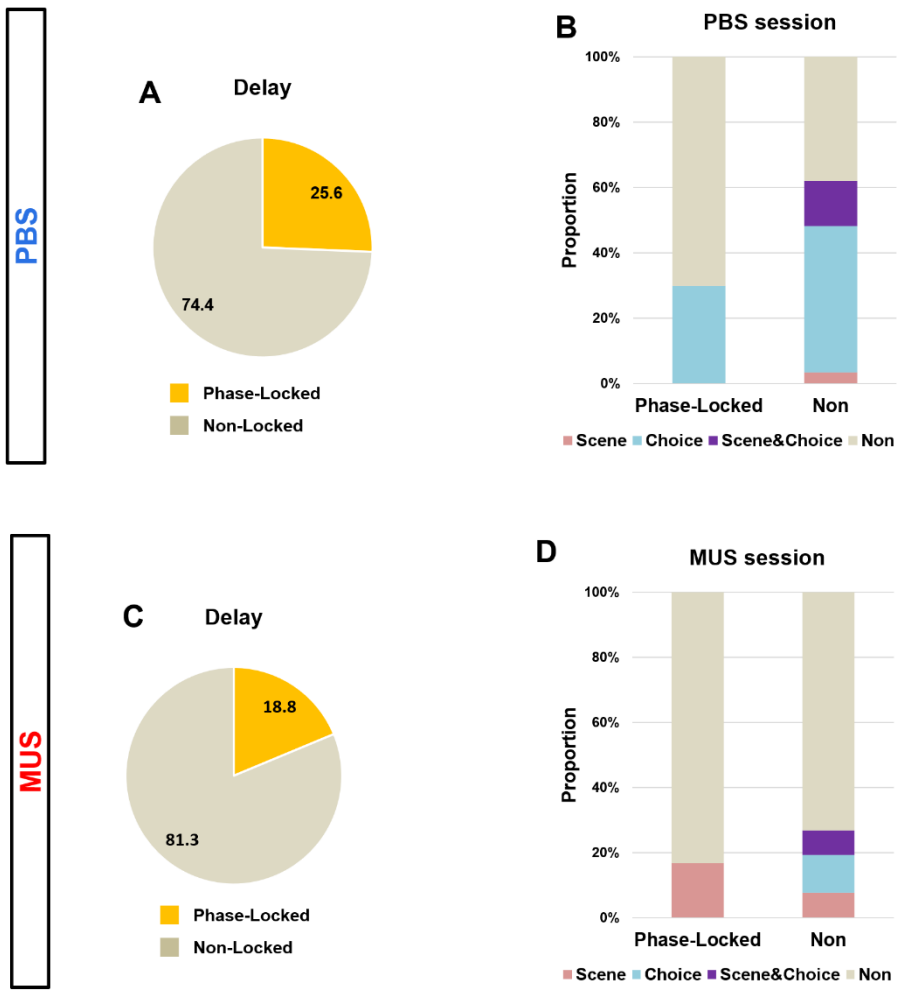

Figure 42. Theta phase-locked cells process the choice information in the delay phase in the IL.

Theta phase-locked cells in the IL show the choice information in the delay phase. Non-locked cells have both choice and scene information. In the MUS session, theta phase-locked cells carry the scene information in the delay phase. The cells which have preferred the theta phase process the scene information, and the choice information is disappeared in the delay phase.

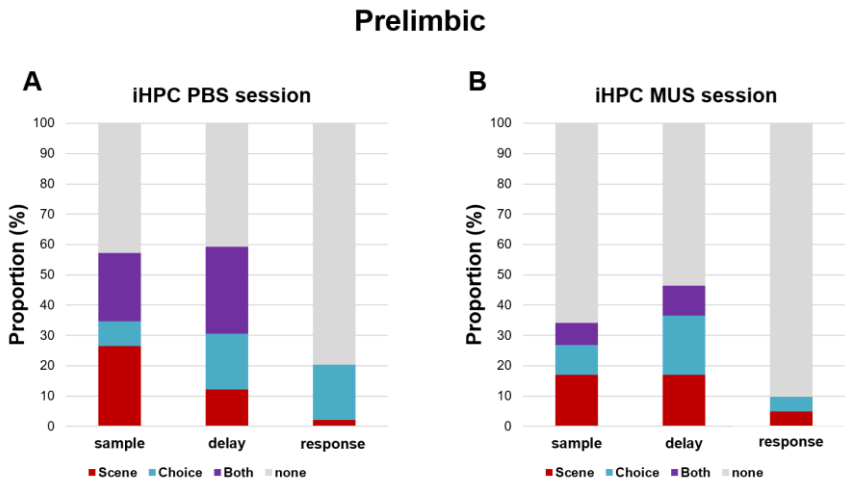

Figure 43. Scene and Choice information processing in the PL cells.

In the sample phase, the scene information (red and purple) mostly disappears, and in the delay phase, most of the scene-associated choice information (purple) is reduced.

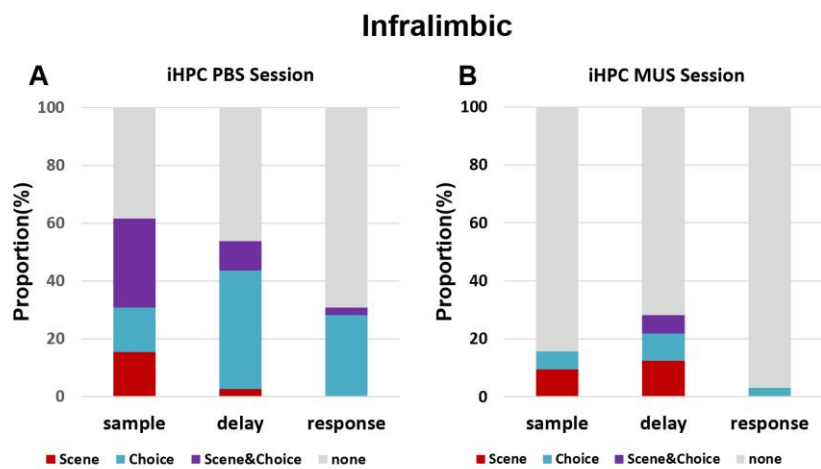

Figure 44. Task-relevant information processing in each phase of the scene-based working memory task in the IL cells.

In the sample phase, the scene-associated choice information (purple) mostly disappears, and in the delay phase, most of the choice information (blue) is reduced.

3.4 Discussion

In the current study, IL is more affected by the iHPC than the PL. Theta power is significantly increased in the delay phase of the task in the IL but not in the PL. Also, the theta phase-locking strength is higher in the delay phase than in the sample phase in the IL. These results indicate that the iHPC to IL circuit is critical in the delay phase. In this delay phase, most of the phase-locked cells in the IL carry the choice information, and this information is disappeared in the iHPC inactivation session. The previous working memory studies did not focus on the iHPC to IL circuit. Those studies targeted the dHPC and PL; nevertheless, there is no direct projection between these areas. I focused on the iHPC to IL network to reveal what information is processed in the direct circuit between the HPC and mPFC. In my study, the iHPC to IL circuit is important for processing the choice information to appropriate action in the response phase. The non-phase locked cells also have task-relevant information in the delay phase. This task-relevant information might come from the dHPC or other cortex areas, for example, the lateral entorhinal cortex (LEC) and perirhinal cortex (Valenti and Grace, 2009; Chao et al., 2015; Hisey and Soderling, 2022). I can not exactly explain why the non-phase-locked cells have task-relevant information, but one thing is for sure, theta phase-locked cells process only the choice information in the delay phase. It is reasonable that in the delay phase, scene-associated choice information is processed to be ready for the response phase. If there is only the scene information in the delay

phase, it can not prepare the appropriate action in the response phase. For this reason, the iHPC project the scene-associated choice information to the IL for the appropriate action according to the environment.

Chapter 4

4.1 Introduction

It is known that the Orbito Frontal Cortex(OFC) is important for processing the reward value signal(Rolls 1996). Schoenbaum et al. (1998) show that the OFC cells encode the expected outcome during olfactory cue-associated learning. In this study, the rat should nose-poke response when the go-signal odor cue is presented. The OFC cells fired during the reward anticipation. The authors suggest that the OFC plays a critical role in the encoding of reward and aversive outcome value for goal-directed behavior. Also, the OFC is known to contribute the working memory (Barbey et al., 2011). The OFC encodes the goals and outcomes in the reward-preference working memory task(Wallis and Miller, 2003). Wallis and Miller (2003) show that the OFC cells encode the reward amount before the response phase. Therefore, the OFC can play an important role in the scene-based working memory task, processing the reward information during the delay phase. There is no direct projection from the iHPC, but the OFC receives the projection from the amygdala and mPFC subregions.

4.2 Results

4.2.1 Histological results

The methods are the same as the chapter 2, but the tetrodes were verified in the OFC in this chapter 4. The tetrodes were mainly positioned in the ventromedial OFC of two rats. The positions of tetrode tips were distributed from +4.7 to +4.2 from the bregma (Figure 45). 73 cells were recorded in a PBS session, and in a MUS session, 50 cells were recorded.

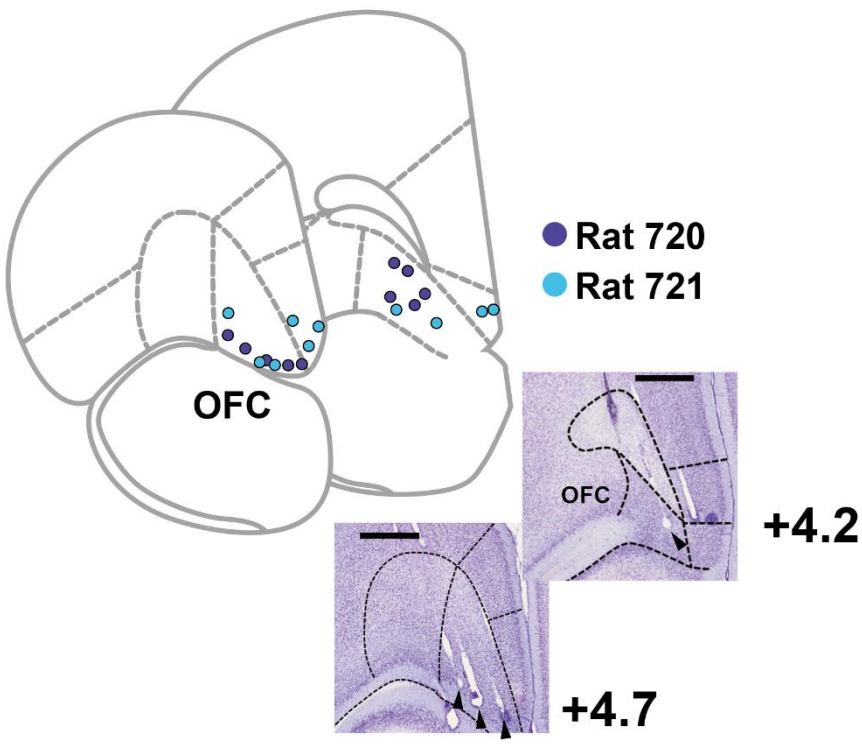

Figure 45. The positions of the tetrode tips were verified.

The tetrode tip positions into the OFC of each rat are verified.

The rat brain atlas is adapted from Paxinos and Watson(2009)

4.2.2 Basic firing properties of the OFC

The number of cells that satisfied the criterion in the OFC is 123 (PBS: n=73; MUS: n=50). To verified the basic cell firing properties in the OFC is not affected by the iHPC MUS sessions, I calculated the peak firing rate(Hz), mean firing rate(Hz), and spike width (μs) in the iHPC PBS and MUS sessions. These basic firing properties between the PBS and MUS sessions are not significantly different (Figure 46 A-D).

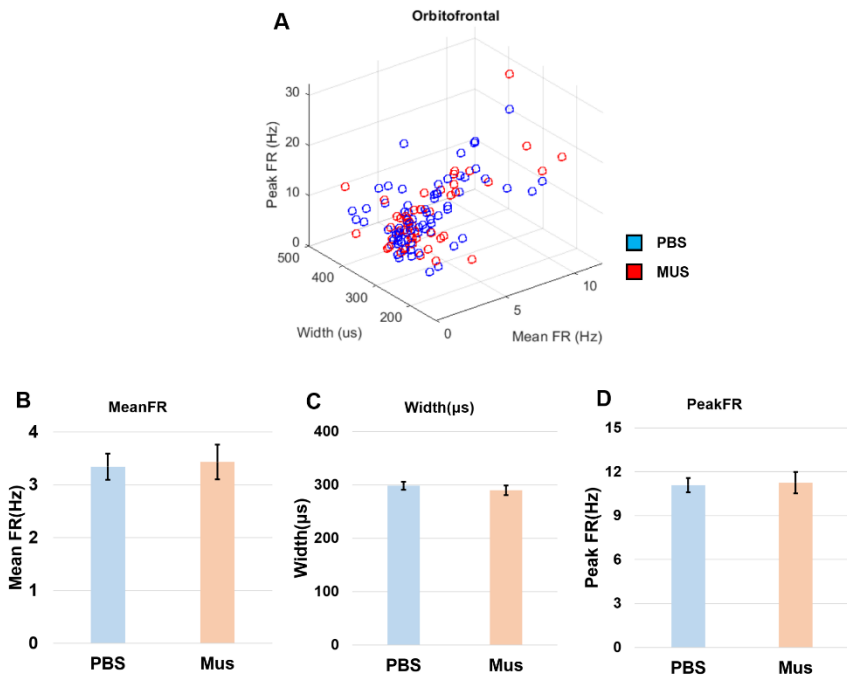

Figure 46. Basic firing properties are not different between the PBS and MUS sessions.

(A) This 3D graph shows the mean firing rate (Hz), the peak firing rate (Hz), and the Width (ms) of the OFC cells. Each dot means one cell. (B) The Mean firing rate (Hz) is not significantly different between the PBS and MUS sessions in the OFC. (C) Spike width(μs) (D) Peak firing rate (Hz).

4.2.3 The OFC cell activities were correlated with choice information in the PBS session but decreased in the MUS session.

The OFC cells showed choice-specific firing rate changes (Figure 47). In particular, the OFC cells activity shows a choice-specific firing rate change and sharply increases the firing rate at the end of the delay phase. When the iHPC CA1 was inactivated, the task-specific correlation and the sharply changing at the end of the delay phase disappear in the OFC. The results of these example cells show that the OFC cells are correlated with the scene and choice information (Figure 48). It indicates that the iHPC is important for the choice of information processing and maintenance in the OFC. RDI was calculated to quantify the difference in rate for each scene and choice. When the iHPC was inactivated, the difference in RDI values with the PBS session in OFC was examined. It shows that the RDIchc value significantly decreased in the sample phase ($Z=4.0137$, $p-val<0.001$, Wilcoxon ranksum test), in the delay phase ($Z=4.3793$, $p-val<0.001$, Wilcoxon ranksum test) and in the response phase ($Z=3.0457$, $p-val<0.01$)(Figure 49,50). However, the scene information is similar between the PBS and MUS sessions in all phases. These results indicate that the iHPC is important for the choice information processing in the OFC.

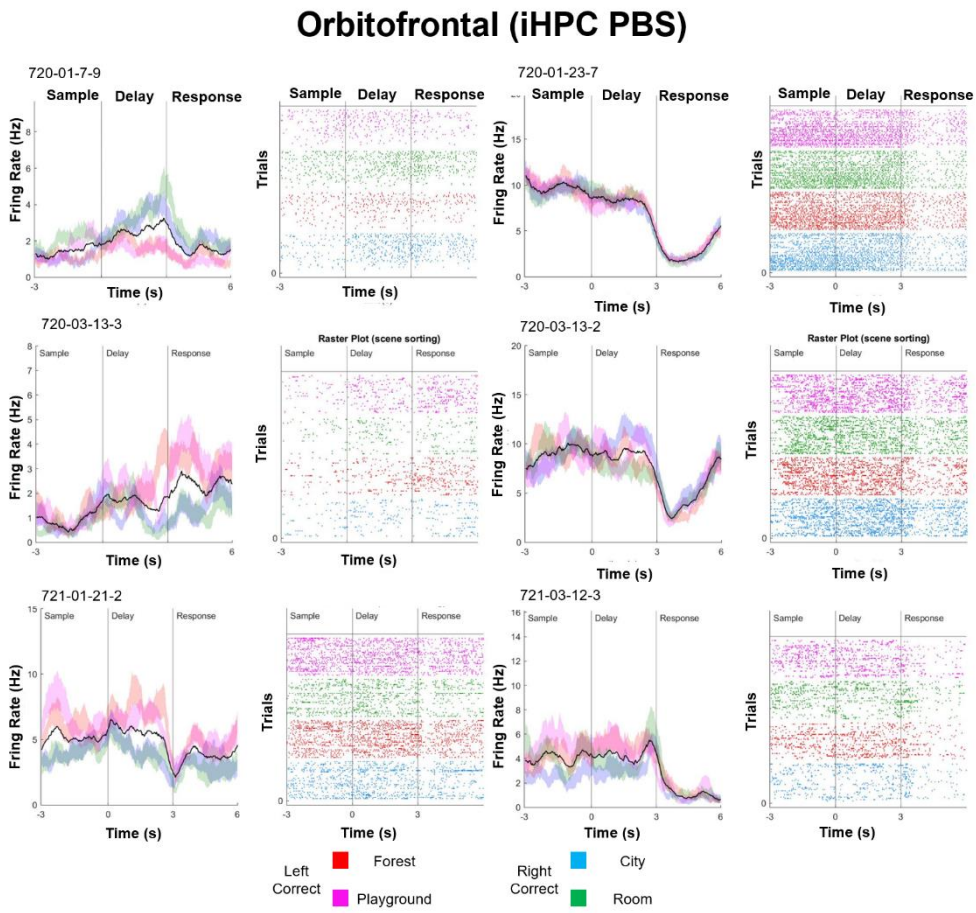

Figure 47. The OFC cells show choice-specific firing rate differences and sharply change the firing rate at the end of the delay phase.

The left column cells show choice-specific firing, and the right column cells show sharply changing activities at the end of the delay phase.

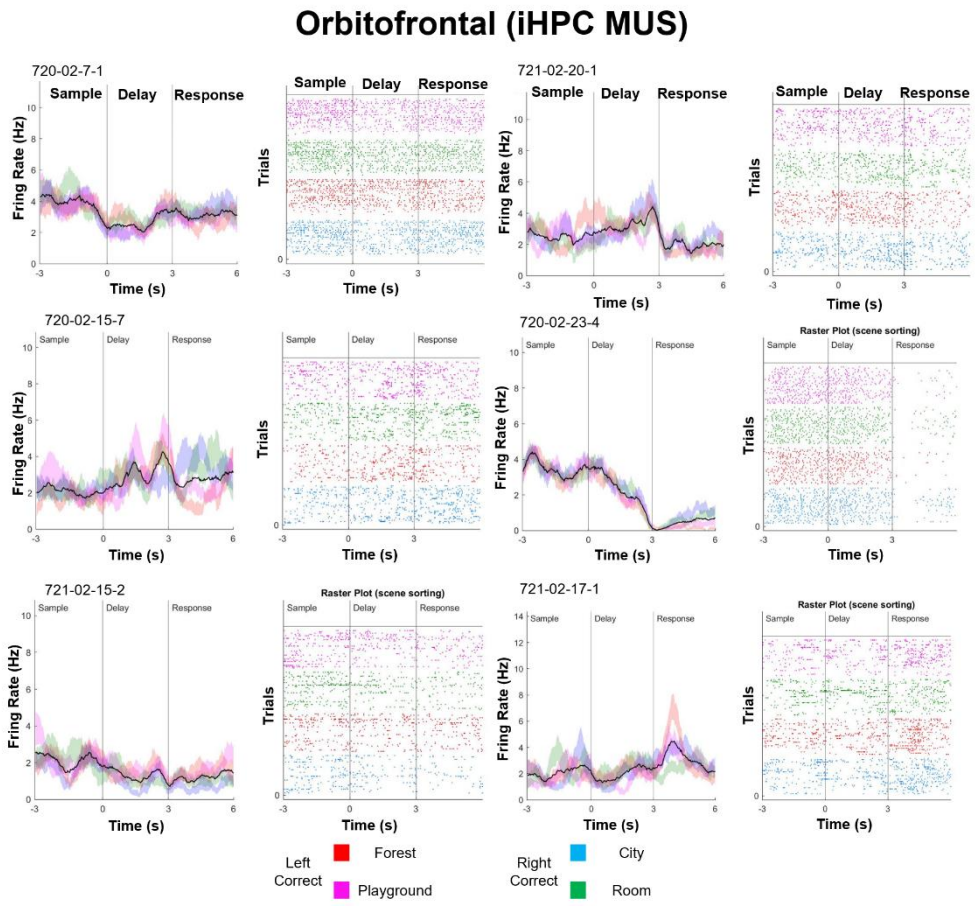

Figure 48. Firing rate differences according to the choice information disappear in the iHPC MUS session in the OFC.

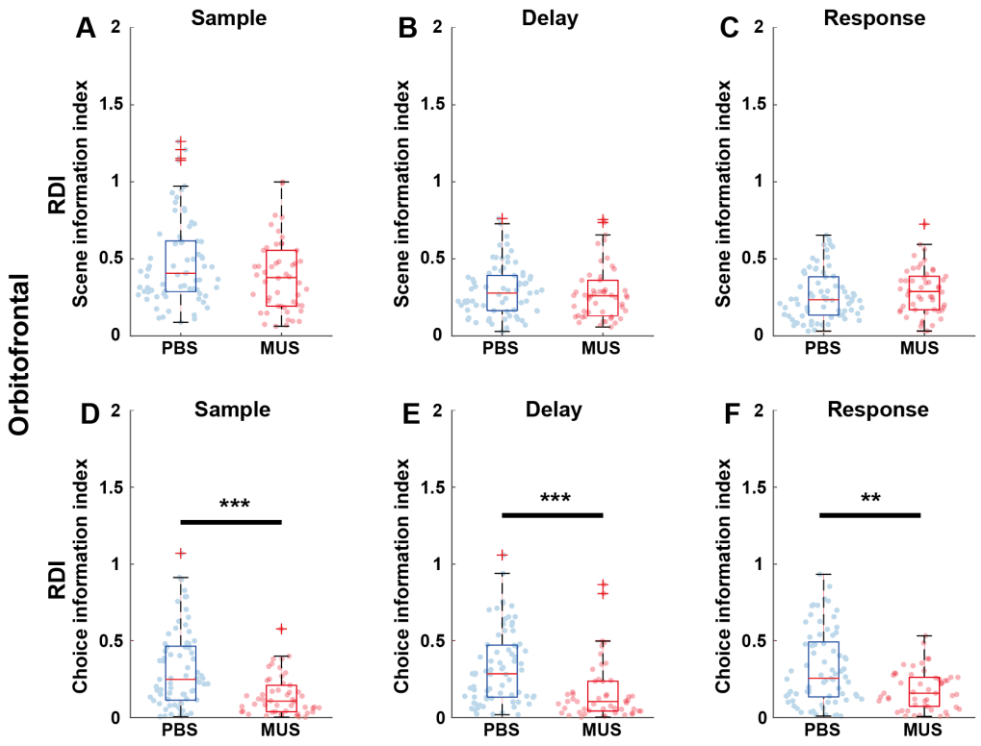

Figure 49. Box plot of the firing rate difference in the OFC.

(A)(D) The choice information is significantly decreased in the sample phase. (B)(E) In the delay phase, the choice information is significantly decreased between the iHPC PBS and MUS sessions. (C)(F) In the choice phase, the choice information is disrupted in the MUS session.

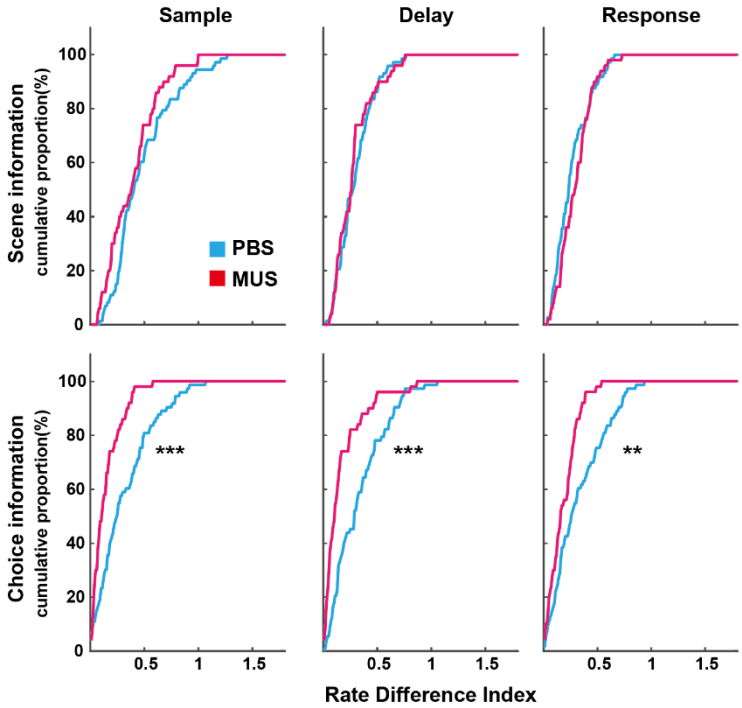

Figure 50. The choice information in all phases is significantly decreased with the iHPC inactivation in the OFC.

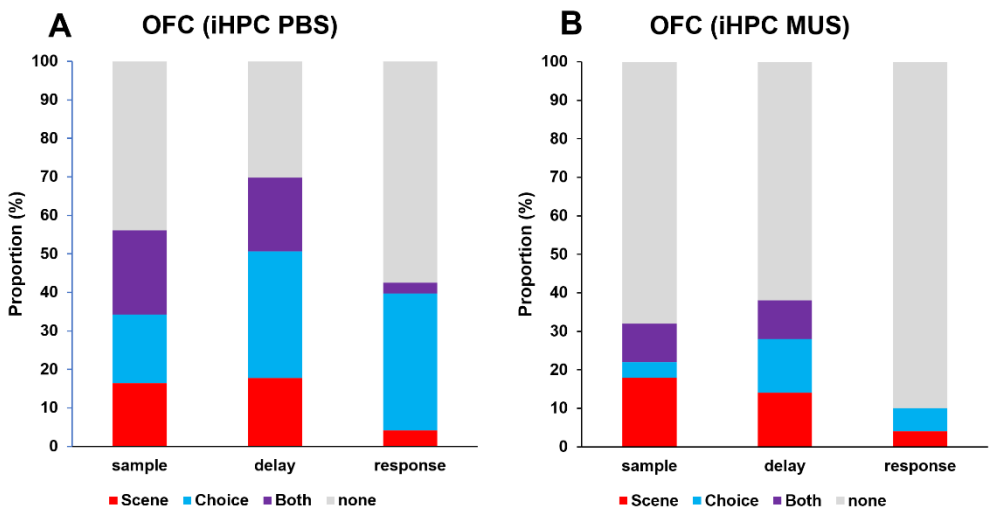

Figure 51. The proportion of the choice information processing cells is decreased in all phases.

(A) The iHPC PBS session. (B) The iHPC MUS session.

4.3 Discussion

In the previous chapters, the PL and IL are the important brain areas processing the scene-associated choice information. These two areas directly receive the information from the iHPC, especially the IL is more affected than the PL. However, the OFC, which has a non-directed connection from the iHPC, shows that only the choice information is disappeared when the iHPC is inactivated. It means the OFC is not important for scene-associated information but important for reward anticipation. There are two types of cells in the OFC, one is a choice information-specific cell, and the other is a highly firing cell during the sample and delay phases. The choice information processing cell can have the reward side information, and the sustained cell can maintain this reward information until the response phase. These two types of cells are disappeared when the iHPC is inactivated. Direct projection does not exist from the iHPC to the OFC, but there is a direct projection from the IL and PL to the OFC. It means the iHPC plays a crucial role in reward anticipation processing in the OFC, but this information can be processed via the PL or IL.

General Discussion

The function of the iHPC in the scene-based working memory task.

The CA1 of the iHPC is a subregion of HPC that has output to the cortex. My experimental results indicate that the information from the iHPC CA1 is the spatial associated value information which is the side of the high-value licking port according to the sample scene. In the real environment, the place-associated value flexibly changes. For survival, the animals should sample the environment and choice the appropriate action based on the associated value. In this process of survival, the iHPC encodes the changing spatial-value information rapidly. The previous study shows that the iHPC is important for the early stage of learning in the water maze task. Also, Burton et al., (2009) concluded that the iHPC plays a critical role in rapidly knowing the value change. This rapid conversion of value information is the base of information for mPFC to perform flexible behavior.

The projection from the iHPC to the mPFC is strongly targeted to the IL, which is the subregion of the mPFC.

Previous studies show that mPFC receives the projection from the MTL area, especially the HPC. It is known that the MTL area is important for episodic memory, scene and object recognition, and place encoding. Especially the HPC plays a critical role in episodic memory and scene reconstruction. In particular, the intermediate part of the HPC is crucial for association and updating the spatial-value information for goal-directed behavior. The iHPC CA1 has a direct projection to the mPFC, but the dHPC does not have a direct projection to the mPFC. However, most of the previous studies

targeted the dHPC to the PL. Therefore, it is possible that the function of the direct projection from the HPC to mPFC was not properly tested in the working memory tasks. For targeting the direct projection from the HPC to the mPFC, I focused on the iHPC to the IL network. Theta frequency is known as an information communicator between the HPC and the other cortex area, especially the PFC. Thus, the mPFC theta power increase indicates the strengthened network between the HPC and mPFC. In the working memory task, theta coherence between the HPC and mPFC increases in the delay phase. Likewise, in my study, the IL theta power increased in the delay phase. This result indicates that the delay phase is the most important phase of working memory in the network of the HPC and PFC.

The function of the iHPC to IL network in the scene-based working memory task.

The IL cells considered as receiving the direct projection from the iHPC have choice information in the delay phase. This choice information is scene-associated choice information from the iHPC known as the place and value association area. Rats were trained to get a reward by choosing the lick port according to the environment. Therefore, rats choose the high-value port on the basis of learning. The iHPC learns and processes the environment associated high-value side of the lick port, and this information is important for the scene-based memory task. For the working memory, the iHPC project the choice information to the IL and maintain the information

along the delay phase. The iHPC and IL communicate by the theta synchrony. The theta phase-locked cells in the IL lose the choice information in the delay phase. It means the IL cells affected by the iHPC directly process the choice information during the delay phase (Figure 51). In the delay phase, there is not shown the sample cues associated with the response. To get a goal, rats should maintain the task-relevant information during the delay phase. Under these circumstances, the iHPC, which has the task-relevant information processing area, and the IL, which maintain the information, work together. Theta phase-locked cells considered to receive the direct projection from the iHPC process the choice information during the delay phase to get a reward after the delay phase. The non-phase-locked cells in the IL also show the scene and choice information in the delay phase. These scenes and choice information might be derived from the LEC, which is one of the MTL areas that directly receives the projection from the iHPC (Cenquizca and Swanson, 2007). The previous study (Chao et al., 2015) shows that the EC and PFC network is important for episodic memory and associative object recognition. This study argues that episodic memory is impaired when the disconnection of the LEC to the mPFC circuit is. Also, another study (Valenti and Grace, 2009) shows that EC projection inhibits the mPFC cell activity in the in vivo study. Thus, the EC to mPFC circuit might be important for sampling the scene in the sample phase.

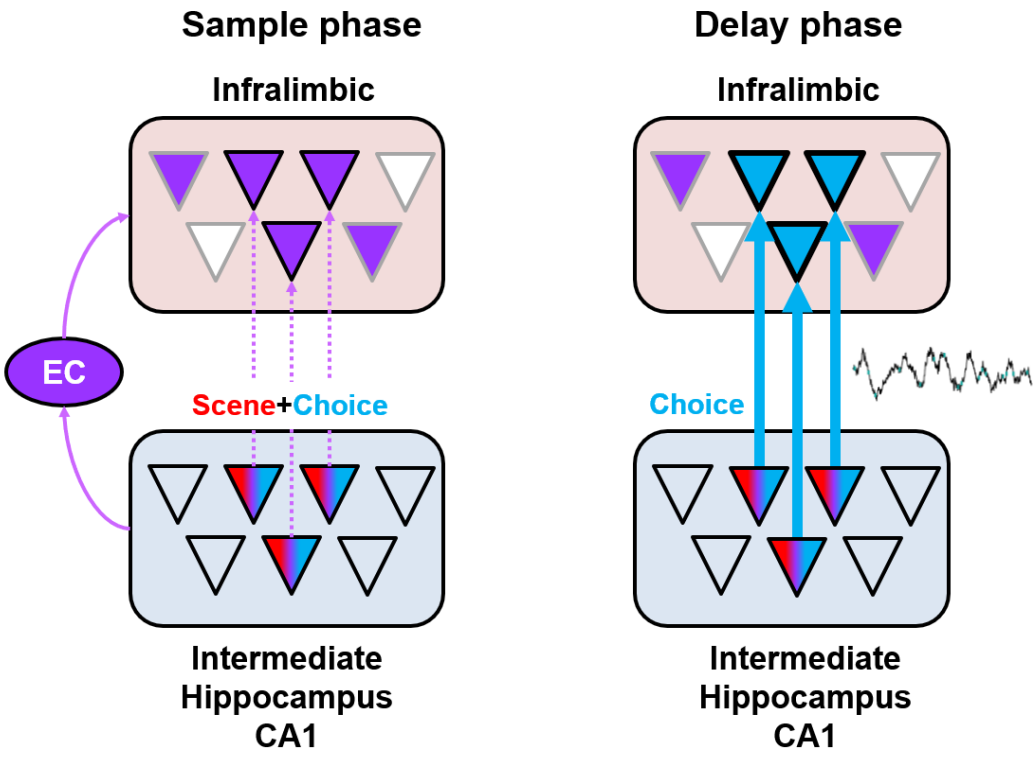

Figure 52. Summary.

In the sample phase, iHPC CA1 does not strongly project to the IL, and also, there might be detour projection through the other area for example the entorhinal cortex (EC). In the delay phase, iHPC CA1 directly projects the choice information to the IL.

The function of the OFC in the scene-based working memory task.

The OFC is known to encode the stimulus-reward association in the goal-directed task. Also, in the working memory task, the OFC lesion decreases performance. Thus, the OFC may play an important role in planning the choice at the response phase after the delay. In my result, the OFC cells significantly decrease not the scene information but the choice information when the iHPC is inactivated. This result indicates that the OFC is important for the planning for the upcoming response phase to get a reward rather than for the processing of the scene information. Previous studies showed that the OFC is important for the stimulus-reward association. However, these results are different from my result. This difference can arise from the difference in the sample cue. The previous studies presented simple sensory cues (i.e., odor cues), but in my study, navigation is an important factor in running in the VR environment. When the rat navigates the environment, the HPC is involved in processing spatial information. In this situation, the OFC, which does not receive the direct projection from the HPC, may not have the scene information. As a result, my study indicates that the OFC processes the upcoming reward anticipatory information during the scene-based working memory task.

Limitation and Future study

In this study, the function of the circuit between the IL and PL was not investigated. When the iHPC is inactivated, the firing pattern of the PL becomes similar to the IL, and the firing pattern of the IL

becomes similar to the PL, suggesting that the reciprocal connection between the two regions affects each other. However, the present study did not confirm this aspect. It is necessary to further investigate the role of the network between the two domains when performing in scene-based working memory. In the RDI analysis, the results are analyzed with all cells in the IL. The number of theta phase-locked cells is not enough for the RDI analysis, so I calculated the RDI value with all IL cells. In future studies, it might be more informative that calculate the theta phase-locked cell's RDI value in the working memory task to know if the IL cell directly projected from the iHPC show the difference in each phase.

It is not clear in my study that the EC input in the sample phase is important for the working memory. Thus, in future studies, it is more informative that test the EC to PFC circuit to verify whether this circuit is important in the sample phase.

Also, in future studies, it can be possible to show the bin-by-bin temporal distribution of the RDI, spatial information score, and decoding accuracy to show how the information dynamically changes in each phase.

Conclusion

In many cases of everyday life, the response phase is separated from the sample phase. For example, we should maintain the goal location during the navigation and take the appropriate action at the goal location. If we can not keep the goal location or make a choice in time, we get bad consequences (e.g., lose the way). Therefore, working

memory is directly related to survival. The mPFC is known as an area of the executive function in goal-directed behavior. However, previous studies have yet to explain what information is processed in the mPFC to conduct the executive function. Also, there needed to be evidence about where the task-relative information came from. To verify the function of the mPFC in goal-directed behavior, I hypothesized that the IL, which is the area directly receiving projection from the HPC, is critical for the scene-based working memory task. In the VR environment, the IL cells maintain the choice information during the delay phase. Also, these firing patterns were disrupted when the iHPC CA1 was inactivated. In these results, I argued that the function from the iHPC to the IL network is preparing the appropriate action in the response phase according to the environment. The iHPC, known as a place-value information association area, projects the scene-associated choice information to the IL, allowing the IL can maintain the choice information even when the scene disappears.

Bibliography

Ahn, J. R., & Lee, I. (2017). Neural correlates of both perception and memory for objects in the rodent perirhinal cortex. Cerebral Cortex, 27(7), 3856-3868.

Ahn, J. R., Lee, H. W., & Lee, I. (2019). Rhythmic pruning of perceptual noise for object representation in the hippocampus and perirhinal cortex in rats. Cell reports, 26(9), 2362-2376.

Baddeley, A. D., & Hitch, G. (1974). Working memory. In Psychology of learning and motivation (Vol. 8, pp. 47-89). Academic press.

Barbey, A. K., Koenigs, M., & Grafman, J. (2011). Orbitofrontal contributions to human working memory. Cerebral Cortex, 21(4), 789-795.

Barthó P, Hirase H, Monconduit L, Zugaro M, Harris KD, Buzsáki G (2004) Characterization of neocortical principal cells and interneurons by network interactions and extracellular features. J Neurophysiol 92:600–608.

Bast, T., Wilson, I. A., Witter, M. P., & Morris, R. G. M. (2009). From rapid place learning to behavioral performance: a key role for the intermediate hippocampus. PLoS biology, 7(4), e1000089.

Burton, B. G., Hok, V., Save, E., & Poucet, B. (2009). Lesion of the ventral and intermediate hippocampus abolishes anticipatory activity

in the medial prefrontal cortex of the rat. Behavioural brain research, 199(2), 222-234.

Carr, M. F., Jadhav, S. P., & Frank, L. M. (2011). Hippocampal replay in the awake state: a potential substrate for memory consolidation and retrieval. Nature neuroscience, 14(2), 147-153.

Chao, O. Y., Huston, J. P., Li, J. S., Wang, A. L., & de Souza Silva, M. A. (2016). The medial prefrontal cortex—Lateral entorhinal cortex circuit is essential for episodic-like memory and associative object-recognition. Hippocampus, 26(5), 633-645.

Cowan, N. (2001). The magical number 4 in short-term memory: A reconsideration of mental storage capacity. Behavioral and brain sciences, 24(1), 87-114.

Eichenbaum, H. (2000). A cortical–hippocampal system for declarative memory. Nature reviews neuroscience, 1(1), 41-50.

Eichenbaum, H. (2017). Prefrontal–hippocampal interactions in episodic memory. Nature Reviews Neuroscience, 18(9), 547-558.

Eichenbaum, H., Dudchenko, P., Wood, E., Shapiro, M., & Tanila, H. (1999). The hippocampus, memory, and place cells: is it spatial memory or a memory space?. Neuron, 23(2), 209-226.

Freedman, D. J., Riesenhuber, M., Poggio, T., & Miller, E. K. (2001). Categorical representation of visual stimuli in the primate prefrontal cortex. Science, 291(5502), 312-316.

Funahashi, S., Bruce, C. J., & Goldman-Rakic, P. S. (1989). Mnemonic coding of visual space in the monkey's dorsolateral prefrontal cortex. Journal of neurophysiology, 61(2), 331-349.

Fuster, J. M. (1997). Network memory. Trends in neurosciences, 20(10), 451-459.

Fuster, J. M., & Alexander, G. E. (1971). Neuron activity related to short-term memory. Science, 173(3997), 652-654.

Hisey, E., & Soderling, S. H. (2022). A prefrontal to lateral entorhinal pathway disrupts memory. bioRxiv.

Hok, V., Save, E., Lenck-Santini, P. P., & Poucet, B. (2005). Coding for spatial goals in the prelimbic/infralimbic area of the rat frontal cortex. Proceedings of the National Academy of Sciences, 102(12), 4602-4607.

Hoover, W. B., & Vertes, R. P. (2007). Anatomical analysis of afferent projections to the medial prefrontal cortex in the rat. Brain Structure and Function, 212(2), 149-179.

Jin, S. W., & Lee, I. (2021). Differential encoding of place value between the dorsal and intermediate hippocampus. Current Biology, 31(14), 3053–3072.

Jung, M. W., Wiener, S. I., & McNaughton, B. L. (1994). Comparison of spatial firing characteristics of units in dorsal and ventral hippocampus of the rat. Journal of Neuroscience, 14(12), 7347–7356.

Keefe, J. O., & Nadel, L. (1978). The hippocampus as a cognitive map. Clarendon Press.

KOLB, B. (1990). Animal models for human PFC–related disorders. In H. B. M. Uylings et al. (Eds.), The prefrontal cortex: Its structure, function, and pathology (Progress in Brain Research, Vol. 85, pp. 501–509). Amsterdam: Elsevier.

Kubota, K., & Niki, H. (1971). Prefrontal cortical unit activity and delayed alternation performance in monkeys. Journal of neurophysiology, 34(3), 337–347.

Lee, C. H., & Lee, I. (2020). Impairment of pattern separation of ambiguous scenes by single units in the CA3 in the absence of the dentate gyrus. Journal of Neuroscience, 40(18), 3576–3590.

Lee, H. W., Lee, S. M., & Lee, I. (2018). Neural firing patterns are

more schematic and less sensitive to changes in background visual scenes in the subiculum than in the hippocampus. Journal of Neuroscience, 38(34), 7392-7408.

Lee, I., & Kesner, R. P. (2002). Differential contribution of NMDA receptors in hippocampal subregions to spatial working memory. Nature neuroscience, 5(2), 162-168.

Lee, I., & Kesner, R. P. (2003). Differential roles of dorsal hippocampal subregions in spatial working memory with short versus intermediate delay. Behavioral neuroscience, 117(5), 1044.

Lee, I., & Kesner, R. P. (2003). Time-dependent relationship between the dorsal hippocampus and the prefrontal cortex in spatial memory. Journal of Neuroscience, 23(4), 1517-1523.

Lee, I., & Solivan, F. (2008). The roles of the medial prefrontal cortex and hippocampus in a spatial paired-association task. Learning & Memory, 15(5), 357-367.

Lisman, J. E., & Grace, A. A. (2005). The hippocampal-VTA loop: controlling the entry of information into long-term memory. Neuron, 46(5), 703-713.

Liu, X., & Carter, A. G. (2018). Ventral hippocampal inputs preferentially drive corticocortical neurons in the infralimbic

prefrontal cortex. Journal of Neuroscience, 38(33), 7351-7363.

MacDonald, C. J., Lepage, K. Q., Eden, U. T., & Eichenbaum, H. (2011). Hippocampal "time cells" bridge the gap in memory for discontiguous events. Neuron, 71(4), 737-749.

Marek, R., Xu, L., Sullivan, R. K., & Sah, P. (2018). Excitatory connections between the prelimbic and infralimbic medial prefrontal cortex show a role for the prelimbic cortex in fear extinction. Nature neuroscience, 21(5), 654-658.

Miller, E. K., Lundqvist, M., & Bastos, A. M. (2018). Working Memory 2.0. Neuron, 100(2), 463-475.

Milner, B. (1963). Effects of different brain lesions on card sorting: The role of the frontal lobes. Archives of neurology, 9(1), 90-100.

Mishkin, M., & Pribram, K. H. (1956). Analysis of the effects of frontal lesions in monkey: II. Variations of delayed response. Journal of comparative and physiological psychology, 49(1), 36.

Morris, R. G., Garrud, P., Rawlins, J. A., & O'Keefe, J. (1982). Place navigation impaired in rats with hippocampal lesions. Nature, 297(5868), 681-683.

Mukherjee, A., & Caroni, P. (2018). Infralimbic cortex is required for

learning alternatives to prelimbic promoted associations through reciprocal connectivity. Nature communications, 9(1), 1-14.

Muller, R. U., & Kubie, J. L. (1987). The effects of changes in the environment on the spatial firing of hippocampal complex-spike cells. Journal of Neuroscience, 7(7), 1951-1968.

Nieder, A., Freedman, D. J., & Miller, E. K. (2002). Representation of the quantity of visual items in the primate prefrontal cortex. Science, 297(5587), 1708-1711.

Norman, D. A., & Shallice, T. (1980). Attention to Action: Willed and Automatic Control of Behavior Technical Report No. 8006.

O'Keefe, J., & Dostrovsky, J. (1971). The hippocampus as a spatial map: Preliminary evidence from unit activity in the freely-moving rat. Brain research.

O'Neill, P. K., Gordon, J. A., & Sigurdsson, T. (2013). Theta oscillations in the medial prefrontal cortex are modulated by spatial working memory and synchronize with the hippocampus through its ventral subregion. Journal of Neuroscience, 33(35), 14211-14224.

Olton, D. S., & Werz, M. A. (1978). Hippocampal function and behavior: Spatial discrimination and response inhibition. Physiology & Behavior, 20(5), 597-605.

Otto, T., & Eichenbaum, H. (1992). Neuronal activity in the hippocampus during delayed non-match to sample performance in rats: Evidence for hippocampal processing in recognition memory. Hippocampus, 2(3), 323-334.

Park, E. H., Ahn, J. R., & Lee, I. (2017). Interactions between stimulus and response types are more strongly represented in the entorhinal cortex than in its upstream regions in rats. Elife, 6, e32657.

Paxinos, G., & Watson, C. (2009). The rat brain in stereotaxic coordinates: compact sixth edition. New York: Academic Press, 143-149.

Pitkänen, A., Pikkarainen, M., Nurminen, N., & Ylinen, A. (2000). Reciprocal connections between the amygdala and the hippocampal formation, perirhinal cortex, and postrhinal cortex in rat: a review. Annals of the new York Academy of Sciences, 911(1), 369-391.

Pribram, K. H., Mishkin, M., Rosvold, H. E., & Kaplan, S. J. (1952). Effects on delayed-response performance of lesions of dorsolateral and ventromedial frontal cortex of baboons. Journal of comparative and physiological psychology, 45(6), 565.

Rolls, E. T. (1996). The orbitofrontal cortex. Philosophical Transactions of the Royal Society of London. Series B: Biological Sciences, 351(1346), 1433-1444.

Schoenbaum, G., Chiba, A. A., & Gallagher, M. (1998). Orbitofrontal cortex and basolateral amygdala encode expected outcomes during learning. Nature neuroscience, 1(2), 155-159.

Scoville, W. B., & Milner, B. (1957). Loss of recent memory after bilateral hippocampal lesions. Journal of neurology, neurosurgery, and psychiatry, 20(1), 11.

Shin, J. D., Tang, W., & Jadhav, S. P. (2019). Dynamics of awake hippocampal-prefrontal replay for spatial learning and memory-guided decision making. Neuron, 104(6), 1110-1125.

Shin, J. D., Tang, W., & Jadhav, S. P. (2019). Dynamics of awake hippocampal-prefrontal replay for spatial learning and memory-guided decision making. Neuron, 104(6), 1110-1125.

Shin,J., Lee,H.W., Jin, S.W., & Lee, I. (2022). Subtle visual change in a virtual environment induces heterogeneous remapping systematically in CA1 but not CA3. Cell Reports, In Press

Siapas, A. G., Lubenov, E. V., & Wilson, M. A. (2005). Prefrontal phase locking to hippocampal theta oscillations. Neuron, 46(1), 141-151.

Sierra-Mercado, D., Padilla-Coreano, N., & Quirk, G. J. (2011). Dissociable roles of prelimbic and infralimbic cortices, ventral

hippocampus, and basolateral amygdala in the expression and extinction of conditioned fear. Neuropsychopharmacology, 36(2), 529–538.

Skaggs, W. E., & McNaughton, B. L. (1998). Spatial firing properties of hippocampal CA1 populations in an environment containing two visually identical regions. Journal of Neuroscience, 18(20), 8455–8466.

Spellman, T., Rigotti, M., Ahmari, S. E., Fusi, S., Gogos, J. A., & Gordon, J. A. (2015). Hippocampal–prefrontal input supports spatial encoding in working memory. Nature, 522(7556), 309–314.

Stuss, D. T., & Alexander, M. P. (2000). Executive functions and the frontal lobes: a conceptual view. Psychological research, 63(3), 289–298.

Tang, W., Shin, J. D., Frank, L. M., & Jadhav, S. P. (2017). Hippocampal–prefrontal reactivation during learning is stronger in awake compared with sleep states. Journal of Neuroscience, 37(49), 11789–11805.

Valenti, O., & Grace, A. A. (2009). Entorhinal cortex inhibits medial prefrontal cortex and modulates the activity states of electrophysiologically characterized pyramidal neurons in vivo. Cerebral Cortex, 19(3), 658–674.

Wallis, J. D., Anderson, K. C., & Miller, E. K. (2001). Single neurons in prefrontal cortex encode abstract rules. Nature, 411(6840), 953-956.

Wallis, J. D., & Miller, E. K. (2003). Neuronal activity in primate dorsolateral and orbital prefrontal cortex during performance of a reward preference task. European Journal of Neuroscience, 18(7), 2069-2081.

Watanabe, T., & Niki, H. (1985). Hippocampal unit activity and delayed response in the monkey. Brain research, 325(1-2), 241-254.

Wood, E. R., Dudchenko, P. A., Robitsek, R. J., & Eichenbaum, H. (2000). Hippocampal neurons encode information about different types of memory episodes occurring in the same location. Neuron, 27(3), 623-633.

Yoo, S. W., & Lee, I. (2017). Functional double dissociation within the entorhinal cortex for visual scene-dependent choice behavior. Elife, 6, e21543.

Zielinski, M. C., Shin, J. D., & Jadhav, S. P. (2019). Coherent coding of spatial position mediated by theta oscillations in the hippocampus and prefrontal cortex. Journal of Neuroscience, 39(23), 4550-4565.

국문초록

해마와 전전두엽 신경 네트워크의 장면 자극 기반 작업기억에서의 기능 연구

박은혜

작업기억은 자극이 사라진 상황에서도 자극에 대한 정보를 유지하는 현상으로 설명되어 왔다. 자극에 대한 정보 유지를 통해 목표 지향적 행동을 수행할 수 있게 되었으며 변화하는 환경에서 필요한 정보를 유연하게 변동할 수 있었다. 이러한 정보를 유지하고 조작하는 기능은 뇌의 전전두엽에서 이루어진다고 알려져 왔다. 원숭이를 사용한 연구들에서는 전두엽 병변 그룹에서 작업기억을 수행하는 것에 문제가 생겼으며, 전기생리학적으로 전두엽의 세포활동을 측정한 결과 지연구간에서 세포 활동이 증가되며 유지되는 것을 관찰하였다. 작업기억을 수행하는 쥐에서도 전두엽이 중요한 역할을 하며, 특히 해마와 전두엽 간의 연결을 차단했을 때 장소 연합 작업기억에 문제가 생겼음을 토대로 이전 연구들에서는 해마와 전두엽이 중요한 역할을 한다고 주장하였다. 그러나 이런 연구들에서는 작업기억이 유지되는 동안 어떤 정보가 유지되고 전달되는지에 대한 분석이 제대로 이루어지지 않고 있으며, 직접적인 연결성이 없는 등쪽 해마와 전변연 피질 사이의 네트워크 연구가 주로 이루어져 왔다. 나는 직접적인 연결성을 가진 중간 해마의 CA1 영역과 변연하 피질의 네트워크에 집중하여 연구를 진행하였다. 두 영역간 정보 전달 매개체로 알려진 세타파가 지연 구간에서 유의미하게 증가하는 것을 확인하였으며, 지연 구간 동안 세타파에 특정 상에 고정되어 활동하는 세포의 대부분이

선택 정보를 가지고 있다는 것을 확인하였다. 이 결과를 토대로 이전 연구들에서 알려지지 않았던 중간 해마와 변연하 피질의 관계가 작업기억의 지연구간에서 중요한 역할을 하며, 특히 선택 정보를 처리하고 있다는 것을 알 수 있었다.

주요어: 전전두엽, 해마, 작업기억, 장면자극기반, 가상현실

Acknowledgment

처음 연구실에 들어왔을 때와 지금의 저를 비교하면, 현재에 이르기까지 많이 깎이고 다듬어져 왔다는 생각이 듭니다. 여러가지로 부족한 저를 대학원 과정동안 지켜봐주시고 지도해주신 이인아 교수님께 감사드립니다.
저에게 좋은 본보기가 되어 주셨던 선배님들과 함께 할 수 있어서 많이 배울 수 있었습니다. 정말 감사합니다. 또한 연구에 열정을 가지고 함께 열심히 일해주셨던 후배님들께 감사드립니다.

제가 가장 힘들었을 때, 연진이가 없었다면 저는 버틸 수 없었을 것입니다. 곁에 남아 힘이 되어주고 무한한 사랑을 준 연진이에게 사랑과 감사를 드리며 맥도날드에서의 결의를 끝까지 실천하겠습니다.

그 동안 도움 주신 많은 분들께 감사드립니다.